NEURAL MECHANISMS UNDERLYING INFORMATION SAMPLING IN MULTIPLE CHOICE DECISION MAKING

CHAN KA SIU

MPhil

The Hong Kong Polytechnic University

2023

The Hong Kong Polytechnic University

Department of Rehabilitation Science

NEURAL MECHANISMS UNDERLYING INFORMATION SAMPLING IN MULTIPLE CHOICE DECISION MAKING

CHAN KA SIU

A thesis Submitted in partial fulfilment of the requirements

for the Degree of Master of Philosophy

August 2022

CERTIFICATE OF ORIGINALITY

I hereby declare that this thesis is my own work and that, to the best of my knowledge and belief, it reproduces no material previously published or written, nor material that has been accepted for the award of any other degree or diploma, except where due acknowledgement has been made in the text.

_____ (Signed)

_____Chan Ka Siu_____(Name of student)

Abstract

In a multifaceted environment, it is common to select among options with uncertain consequences or outcomes. Often the uncertainty can be reduced by sampling information, such as gathering information from options and searching for new options. In other words, there are at least two ways in which we can sample information. Existing literature has discussed the option selection and information sampling processes independently. However, there is a lack of a unified framework to illustrate the dynamics between them, while these three decision-making processes should be considered at the same time.

In **Chapter 1**, I illustrate a daily life example and state the importance of investigating the neural mechanisms of information sampling in multiple-choice decision-making. To address the major problem in this thesis, I reviewed three candidate brain regions: the ventromedial prefrontal cortex (vmPFC), the anterior cingulate cortex (ACC), and the intraparietal sulcus (IPS). The vmPFC is related to both valuation and value-comparison processes, which are essential in selecting better options. The former process allows us to assign an internal value to an option, while the latter process allows us to make the comparison between options according to their values. The ACC is related to searching for new options from the environment, while the IPS is related to uncertainties and information gain.

I then designed a multiple-choice decision-making task with three possible decisions (i.e., to accept a current option; to clarify a current option; to search for new options) to investigate both computational and neural mechanisms of information sampling in **Chapter 2 & 3** respectively. Behavioural results are discussed in **Chapter 2**. During the designed decision-making task, while the value of existing

options was greater , but the outcome was largely uncertain at the same time, clarify decisions were more preferred. While the value of searching was greater, search decisions were more preferred. These results served as a fundamental framework to illustrate the sampling of information from existing options and the environment involved different mechanisms. In **Chapter 3** I report a functional magnetic resonance imaging (fMRI) experiment to examine the neural signals of the vmPFC, IPS and ACC. The results show that during multiple-choice decision-making, the vmPFC guides the selection of the best option. Critically, the IPS and ACC were found to be crucial during information sampling. The IPS signals the demand for information and information gain, which guide clarify decisions to reduce uncertainty, while the ACC signals the incentive of searching, which guides search decisions.

After the vmPFC, IPS and ACC were found to be involved in information sampling during multiple-choice decision-making, how these three regions formulated final decision was still not clear. To address this problem, in **Chapter 4** I employ a convolutional neural network (CNN), which is a deep learning technique that is trained and dependent on human data, without any prior assumptions (model-free) to predict human decisions. The CNN involves feature extraction, integration and decision-making processes, which are particularly important in the decision-making task. By conducting a series of representational similarity analyses (RSA), which is multivariate analysis that allows us to compare the representational similarities between the multimodal representations in the CNN and the multi-voxel activation patterns of the human brain, which helps us better understand the computational processes in our brains. I demonstrate that the IPS, ACC and vmPFC are related to the early, intermediate, and late stage of decision formation respectively.

To conclude, I demonstrate that the IPS is critical during the sampling of information from options, the ACC is important during the sampling of information from the environment to discover alternatives, while the vmPFC operates as a guide to stop sampling information and accept existing options. The unified framework to illustrate the dynamics between option selection processes and information sampling processes was demonstrated.

Acknowledgements

I would like to express my gratitude to the following people who have been supporting instrumental in my completion of Master of Philosophy.

First and foremost, I would like to extend special thanks to my supervisor, Dr Bolton Chau, for his unwavering guidance and support throughout my academic journey. Despite not being his student initially, he generously offered his time to speak with me, providing invaluable advice and inspiration that helped me to think beyond the traditional framework. His patience and unwavering support have been crucial in encouraging me to persevere during challenging times, and I consider it a privilege to have been his student.

Thanks to my colleague, Dr. Kelvin Law, for providing me with a wealth of resources that allowed me to quickly grasp new concepts and techniques. His experience as a research student has been invaluable, and he has always been a source of encouragement and motivation during times of frustration and disappointment.

Thanks to my mother, Ms. Michelle Poon, for her financial support and understanding, which allowed me to focus on my studies without the added burden of financial pressure.

Table of contents

Chapter 1: Introduction

Imagine that you are shopping on eBay – you might need some time to find the best product that suits your needs due to the overwhelming amount of information presented on the screen. This information includes the price, features, and appearance, among other things, which require careful consideration. During this process, there are three critical decisions that you might make. The first decision is to search for new products. Initially, you might scroll through the webpage to gather more available alternatives, or you risk missing out on some good products as they might be displayed on other pages. The second decision is to clarify the products that have been searched. This involves reading the product information that is unclear or limited. If we do not clarify the information, the products may not be suitable for your needs. Both the search and clarification decisions (i.e., information sampling) are essential for selecting better options and achieving better outcomes. After a series of information sampling, you might make the third decision, which is to accept among the current products and make a purchase. Although the process of deciding between these three decisions is common in our daily lives, there is a lack of a unified framework to illustrate their dynamics. The neural mechanism of information sampling in multiple-choice decision-making is still not entirely clear, and it is vital to study this mechanism as it provides a better understanding of how our brains operate during information sampling.

1.1 Value-based Decision-making

It is crucial to understand how we determine that current products are not appealing enough, which then motivates us to sample more information. This involves two processes: the valuation process and the value comparison process.

First, we need to understand the "values" of current products, which are constructed by factors such as price, functions, appearance. The valuation process allows us to assign an internal value to objects subjectively. However, the results of this process can vary between individuals, as we can have different preferences for the same product. Second, we need to compare the values of current products with our expectations of sampling new products. This is called the value comparison process, which enables us to choose a better option among multiple products. In most cases, we make decisions based on the expected future reward, usually selecting the option with the greatest expected value among multiple options (Montague et al., 1996). Expected value takes both the outcomes and the likelihood (or probability) into account to guide decision-making. For example, when choosing among two gambles, one that offers a 0.3 probability of winning $200 and another that offers a 0.5 probability of winning $20, most people will choose the first gamble because its expected value of $60 (winning amount $200 multiplied by its probability of 0.3) is greater than the expected value of the second option, which is $10 (winning $20 multiplied by its probability of 0.5).

The valuation and value comparison processes play crucial roles in value-based decision-making by allowing us to assign internal values to different products

and compare those values to choose the best option. These two processes are suggested to occur simultaneously (Albantakis & Deco, 2009; Wang, 2002).

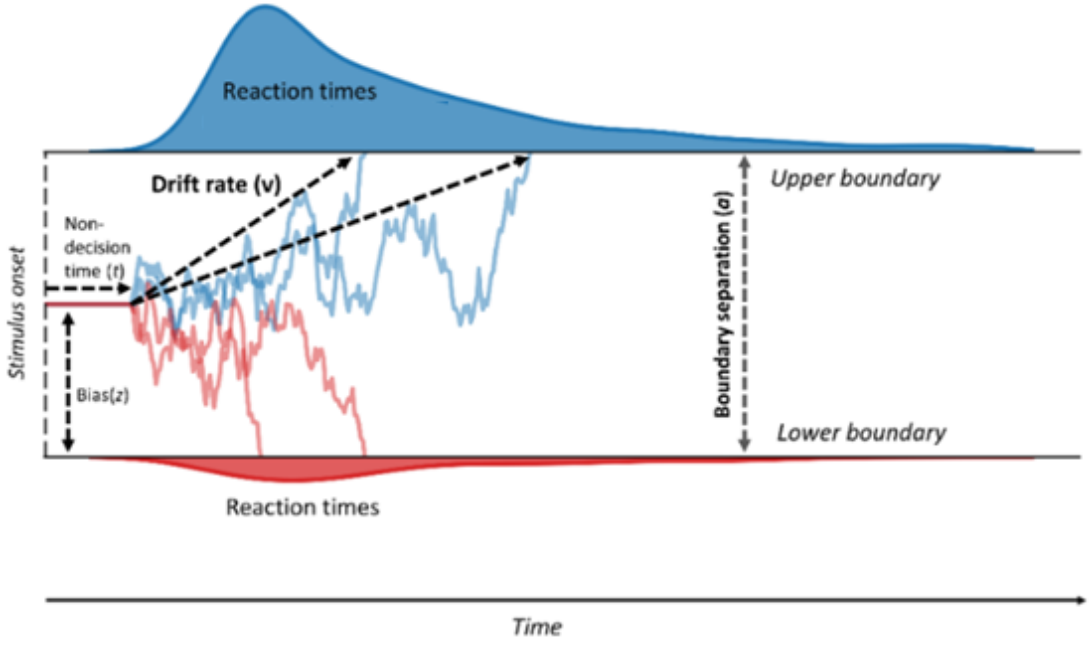

Figure 1. The conceptual model of the drift-diffusion model (DDM) suggests the stochastic nature of our decision-making process. It has been widely used to understand the mechanism of binary-choice decision problems, and incorporates the reaction times and the randomness of the choice pattern. It proposes that decisions are made when the evidence accumulation reaches a stopping boundary (upper or lower, which represents one of the available decisions or options). Evidence accumulation is depicted by the drift rate over time. Adapted from Vinding et al. (2021).

The concept of making decisions based solely on optimal expected value is not always applicable in real-life scenarios such as choosing meals among multiple options. To better explain how sophisticated and stochastic our decisions could be, the drift diffusion model (DDM) is commonly used in psychology and neuroeconomics to explain binary-choice decision problems. This model considers evidence

accumulation in both options until a stopping boundary is reached, at which point a decision is made. The process of evidence accumulation can be influenced by discrepancies between options, including their values. For instance, it takes a short time for evidence accumulation when there is a significant value difference between two options. However, it takes a longer time for evidence accumulation when there is just a tiny value difference. Apart from value difference, the certainty of an option is also a kind of evidence, which could be the probability of gaining rewards. At the same time, the range of the discrepancy also implies task difficulty. A tiny discrepancy implies an immense task difficulty so that a longer time is needed for consideration. The task difficulty could be observed by the relationship between choice accuracy and response time, and it has been suggested that making a corrected response takes less time than an uncorrected response (Drugowitsch et al., 2012; Milosavljevic et al., 2010). While DDM offers insight into sophisticated and stochastic decision-making, it has limitations, including its inability to address non-binary decision problems and its unrealistic assumptions, such as both the volatility of the signals and the cost of sampling are constant over time (Edwards, 1965; Ratcliff, 1978), which is biologically unrealistic (Wang, 2002).

Value-based theories are still powerful tools for understanding diverse scenarios of decision-making. They provides a foundation for investigating the underlying mechanisms of decision-making. For instance, this could also help to identify which brain regions are related during decision-making by correlating both the values and brain activities. Although this approach has been widely used in decision neuroscience over the decades, there was a lack of biological evidence about how the process of decision formation occurred in our brains and neurons.

The Biophysical model is another decision-making model that simulates neural activities during both the valuation process and the value comparison process (Wang, 2002). It demonstrates how both valuation and value comparison processes occur in neurons, providing more biological evidence. This model has been suggested to have a similar mechanism to human brain activities during decision-making, and has been used in decision neuroscience to identify brain regions related to decision-making (Bonaiuto et al., 2016; Hämmerer et al., 2016).

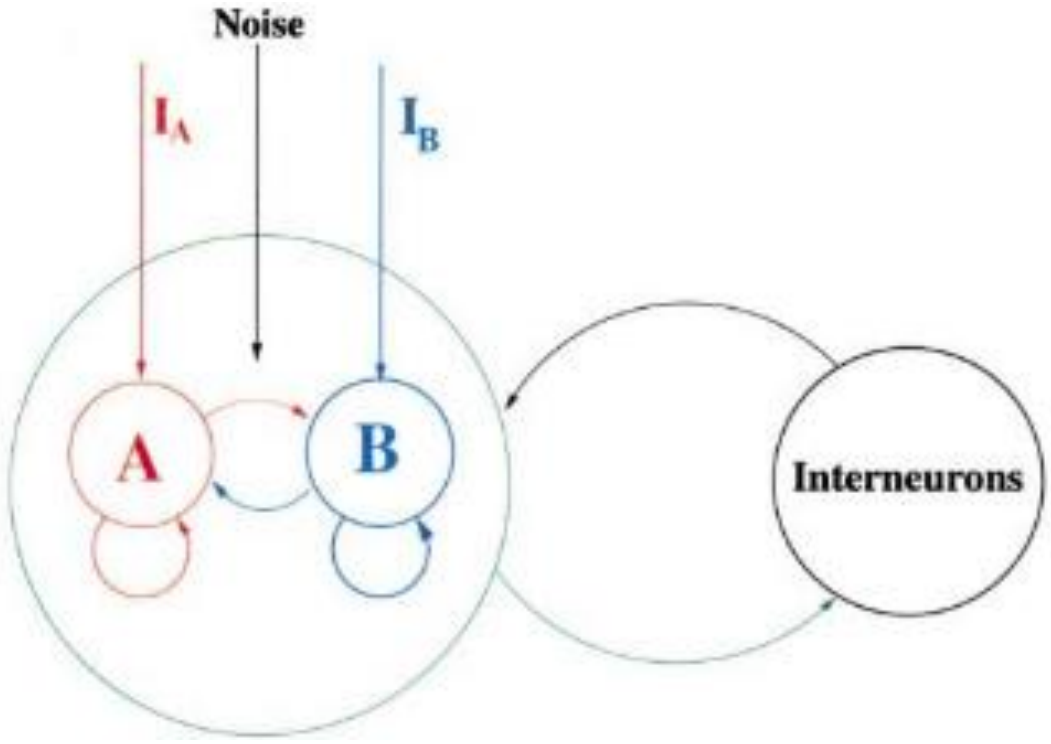

Figure 2. The conceptual model of the Biophysical model in 2002. This model was used for simulating neural activities during binary-choice decision problems. The two pyramidal cell groups (A and B) represented two stimuli, where the valuation process occurs. The interneurons provided inhibition feedback that regulated the activities of both pyramidal cell groups as the value comparison process. Adapted from Wang (2002).

This model comprises of two pyramidal cell groups with strong recurrent excitatory connections that receive the value of corresponding stimuli (Wang, 2002) (Fig. 2). The valuation process is simulated by a positive correlation between the value of stimuli and the activity of each cell group. Thus, a larger value input results in a more prominent activity in the cell group. Besides, the comparison process is simulated by inhibition feedback from interneurons, which regulates the activities of both pyramidal cell groups. For instance, all pyramidal cell groups can indirectly suppress each other by their input sent to the interneurons. As a result, the cell group with the largest value input will have the most prominent activity, inhibiting the other cell groups. Ultimately, a cell group with the prominent firing rate state would be selected by the model indicating the choice.

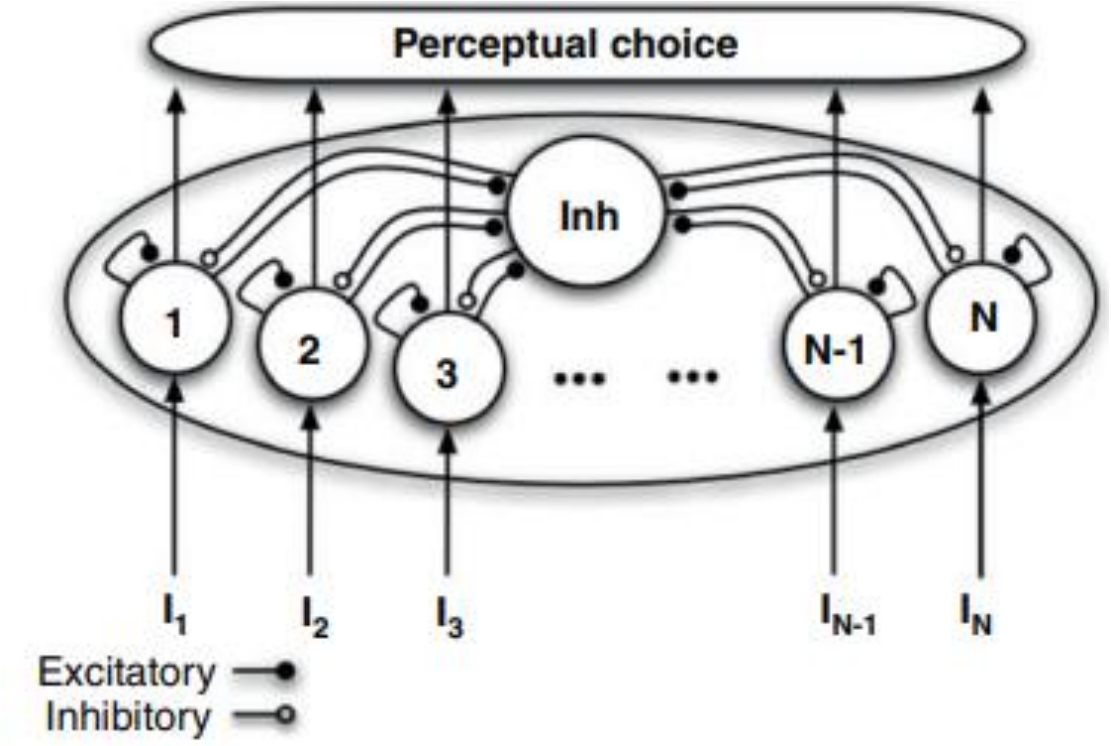

Figure 3. Conceptual model architecture of the Biophysical model in 2012. This model was used for simulating neural activities during multiple-choice decision

problems. There could be N pyramidal cell groups which represent multiple stimuli. Adapted from Wang (2012).

The Biophysical model demonstrates how both valuation and value-comparison processes could biologically occur in neurons to guide decisions. It was later found to be capable of solving multiple-choice decision problems by adding extra pyramidal cell groups (Wang, 2012) (Fig. 3). However, it assumes unlimited working memory , which are feasible to occur in our brains. Also, the model lacks the ability to consider non-option value information that might influence our decisions such as the searching cost and the incentive to search. Overall, the Biophysical model suggests that neural activities are predictable and associated with the value information with more biological evidence.

Indeed, both valuation and value comparison processes are essential for making value-based decisions, which allow us to understand the options and make a comparison between them to achieve better outcomes. However, in our daily life, it is ubiquitous to select among multiple options with uncertainties. The uncertainty might influence the results of the valuation process since we can only rely on limited information to assign values to options subjectively. Thus, the results of the value comparison process that guide final decision-making would also be influenced. In other words, our expected outcomes would be more unpredictable if the options are largely uncertain. However, we could reduce the uncertainty through information sampling.

1.2 Information Sampling

Shopping on eBay is an example of how information sampling is important, which has been mentioned in Chapter 1. This daily life example illustrates that we can sample information from both options and the environment by reading the product information and searching for new products, respectively. Sampling from options allows us to reduce the uncertainties, while sampling from the environment allows us to discover more alternatives. However, these processes could also be sophisticated and stochastic (Blanchard & Gershman, 2017). For instance, it has been suggested that the strategies of how we sample information and what to sample are still under debate (Gottlieb, 2018).

First, information sampling might include a series of accept and reject decisions (Freidin & Kacelnik, 2011; Pearson et al., 2014). For instance, when shopping on eBAy, my might switch between staying and scrolling down the screen. This process could continue infinitely unless we find a product reaches or approximately reaches our optimal expected value (Tervo et al., 2021). However, there is a trade-off between the time cost and non-stop searching, and the risk of failing to accept a good product.

Second, the uncertainty-driven sampling strategy suggests that the drive to search came from the belief in some better alternatives which have not been discovered in the environment (i.e., searching and information bonuses (Wilson et al., 2014), and the “uncertainty” about future outcomes (Badre et al., 2012)). Uncertainty arises when we have imperfect or unknown information about both the options and the environment (Hubbard, 2014). The extent to which the information we have varies

with our certainty toward the options, which can lead to lower decision confidence (Hebscher & Gilboa, 2016; Shapiro & Grafton, 2020). Although we can reduce the uncertainty of the environment by searching for more alternatives, we still lack certainty about the existing options. It is not sufficient to achieve better outcomes by just searching for alternatives since we are not "omniscient" but can only rely on the information that we have in order to select the better ones. To address this, we can also reduce the uncertainty of the options by exploiting or re-sampling them (Reitich-Stolero et al., 2019). In other words, we can sample information from a current product (i.e., to clarify something), such as reading its details or searching for some comments about it to reduce the uncertainty.

Third, interestingly, the random sampling strategy suggests that consideration of future reward and long-term planning may not be necessary (Knox et al., 2011). Although it seems that many information sampling strategies have been proposed and suggested, the specific strategy adopted by humans is still under debate (Blanchard & Gershman, 2017). Meanwhile, information sampling strategies have been suggested that might change over time. For instance, the threshold from accepting the preferred options rather than searching for more alternatives can be changed. However, it would be concurrently adopted before a new set strategy is formed (Donoso et al., 2014; Mooney & Cleland, 2001).

The aforementioned strategies show how information sampling can be sophisticated and stochastic (Blanchard & Gershman, 2017). Besides, various factors have been suggested as potential influences on our preference to sample information, for instance, the expected value of the sampling environment (Hunt et al., 2012; Juni, Gureckis & Maloney, 2016); the expected value difference between the currently

available options and the environment (Raiffa & Schlaifer, 1961); the sampling cost, which could be time and money (Juni et al., 2016); and the number of alternatives that are available to sample (Kolling et al., 2018). At the same time, there are also factors that may encourage us to sample information, such as when we are new to an environment, which allows us to gain more information (Wilson et al., 2014; Zajkowski et al., 2017); when we have higher expectations of future outcomes and a greater chance of obtaining the maximum value (Blanchard & Gershman, 2017); or when we want to confirm our prior beliefs (Hunt et al., 2016).

In the last decade, the neural mechanisms underlying information sampling have been explored. Various brain regions associated with information sampling have been identified, including the intraparietal sulcus (IPS) (Horan et al., 2019) and the anterior cingulate cortex (ACC) (Kolling et al., 2012, 2018). However, the IPS and the ACC are mainly identified during the sampling of information from options and the environment, respectively. These two types of information sampling may involve distinct neural mechanisms. Although people usually engage in both types of information sampling simultaneously, previous literature have tended to investigate these two processes independently rather than examining them in a single study. There is a lack of a unified framework to elucidate the dynamic between these two types of information sampling.

In addition to the IPS and ACC, which have previously been found to be related to information sampling, the ventromedial prefrontal cortex (vmPFC) is also suggested to play a critical role in value-based decision-making through its involvement in both valuation and value comparison processes. As such, it is likely to also be involved in information sampling. In this thesis, I define the vmPFC, ACC

and IPS as the candidate regions to investigate their roles in information sampling during multiple-choice decision-making. Further details regarding these three regions will be discussed deeply in-depth sections 1.3, 1.4 and 1.5.

1.3 Ventromedial Prefrontal Cortex

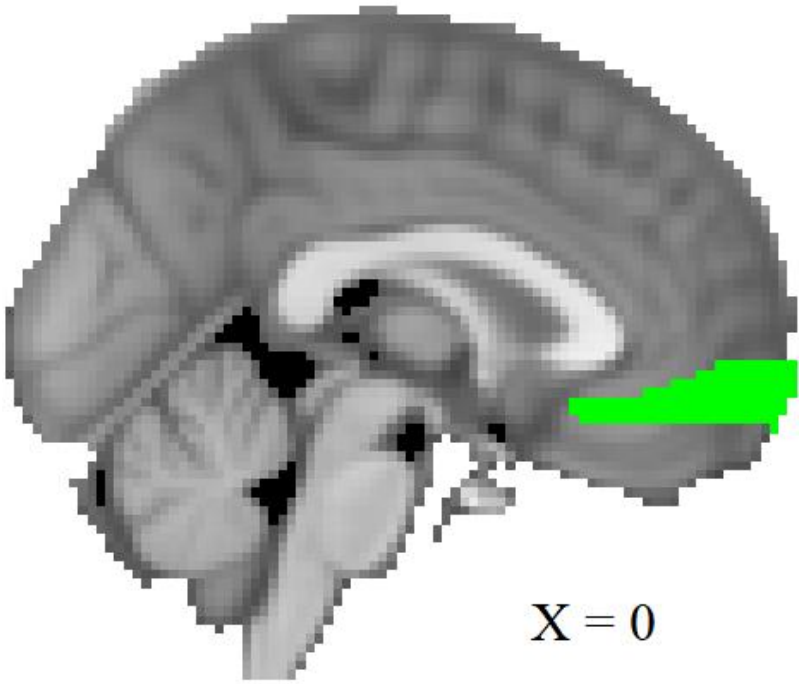

Figure 4. The ventromedial prefrontal cortex (vmPFC). The cluster of the vmPFC (green) was extracted from the Automated Anatomical Labelling Atlas 3 (Rolls et al., 2020).

The vmPFC was the first candidate region to be investigated in this study (Fig. 4). It is situated in the prefrontal cortex and generally encompasses Brodmann's areas 10, 14, 25, and 32 (Bartra et al., 2013). However, some lesion studies about the vmPFC might also include Brodmann's areas 11, 12, 13. The boundaries of the vmPFC, therefore, are still being debated (Lopez-Persem et al., 2019).

The vmPFC has been widely studied in various domains such as emotion regulation, i.e. the ability to control and avoid negative behaviours such as drug abuse

arising from uncomfortable and painful emotions (Hänsel & von Känel, 2008; Pessoa, 2008); memory consolidation, i.e. the ability to undertake cognitive tasks (Bonnici et al., 2012; Bontempi et al., 1999; Frankland & Bontempi, 2005); and especially valuation system and decision-making (Hunt et al., 2012; Lebreton et al., 2009; Levy & Glimcher, 2012; Strait et al., 2014).

The vmPFC is crucial in both valuation and comparison processes (Hunt et al., 2012; Jocham et al., 2012; Strait et al., 2014), which involves evaluating options and making comparisons among them. Indeed, these processes could be subjective. For instance, we might hold different values toward an apple and an orange, and we can select differently after we make a comparison according to our valuation of both options. Indeed, the vmPFC has also been found to be related to modulating subjective value (Bartra et al., 2013; Levy & Glimcher, 2012). Meanwhile, previous studies have suggested that the vmPFC encodes expected value, which is one's expectation of potential future reward, usually calculated by the reward magnitude and possibility (Blair et al., 2006; Gläscher et al., 2009; Hampton et al., 2006); and making value-guided decisions (Kable & Glimcher, 2009), as it could signal the value difference between options in both binary (Fellows, 2011; Rangel & Hare, 2010; Rudebeck & Murray, 2011) and multiple-choice decision-making (Boorman et al., 2013), which also demonstrates the flexibility of the vmPFC in value-based decision-making.

To showcase the flexibility of the vmPFC from binary to multiple-choice decision-making, Boorman et al. (2013) adopted a sequential multiple-choice decision-making task for human participants. The participants were asked to make the first decision among three options. In some conditions, they made the second decision

among the remaining two options after the first option was selected. They found that the vmPFC positively encoded the value of the best option but negatively encoded the value of the next best option (Boorman et al., 2013). Critically, after the first selected option was removed, the vmPFC could then positively encode the value of the current best option during the second decision (which was the second-best option during the first decision). Since the unchosen option in both first and second decisions was negatively encoded by the vmPFC, the result supported that the vmPFC displayed its flexibility in encoding value difference signals (the value of the chosen option minus the unchosen option) in both binary and multiple-choice decision-making tasks. However, the value difference signal in the vmPFC would be influenced by the value of distractors, which are irrelevant options during decision-making. The value difference signal was found to be stronger in the vmPFC when there was a distractor with a greater value (Chau et al., 2014).

To conclude, the vmPFC plays a critical role in both valuation and value comparison processes, such as encoding the expected value and making comparisons among multiple options. Its flexibility in the valuation process concerning the best option from binary to multiple options. To study the neural mechanisms of information sampling during multiple-choice decision-making, the vmPFC was one of the candidate regions to be focused on.

1.4 Anterior Cingulate Cortex

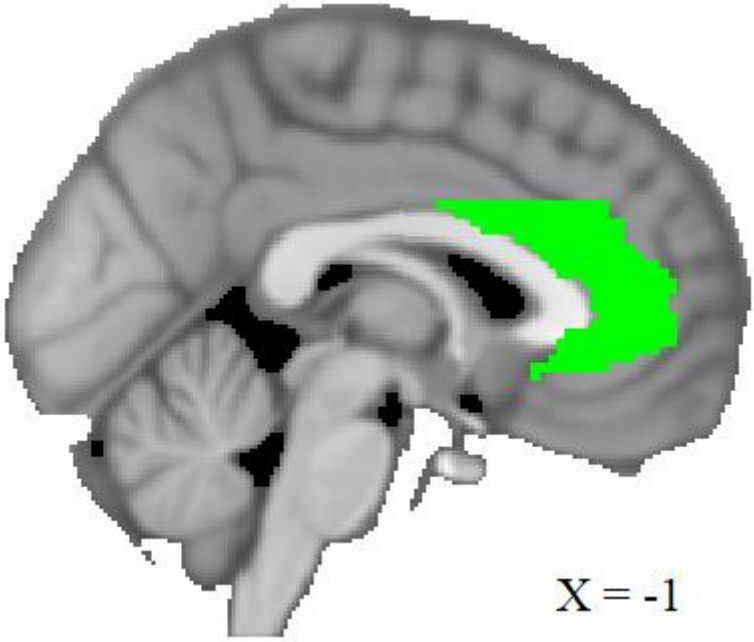

Figure 5. The anterior cingulate cortex (ACC). The cluster of the ACC (green) was extracted from the Automated Anatomical Labelling Atlas 3 (Rolls et al., 2020).

The ACC was the second candidate region to be investigated in this study (Fig. 5). It includes Brodmann's areas 24, 25, 32, and 33 (Paholpak & Mendez, 2016; Palomero-Gallagher et al., 2009), which is situated in the medial part of each cerebral hemisphere, adjacent to the posterior cingulate cortex (PCC) (Stevens et al., 2011). It is also connected to both the limbic system and prefrontal cortex (Stevens et al., 2011), which also plays a critical role in affect-regulation and cognitive tasks.

The ACC is comprised of five sub-regions (Beckmann et al., 2009; Margulies et al., 2007). For instance, the dorsal anterior cingulate cortex (dACC), one of the sub-regions of the ACC has been suggested to play a critical role in reward-based decision-making (Bush et al., 2002). It facilitates the future events by integrating information and moderates the adjustment of behaviour in response to new

information (Behrens et al., 2007; Quilodran et al., 2008; Wessel et al., 2012). It is also associated with reward-seeking behaviour (Kurniawan et al., 2013). For instance, adaptation from a known environment to exploring a new environment with a greater expected value. Studies on foraging choices have also found that the ACC encodes the cost and the value of searching (Kolling et al., 2012, 2018). And the cost of searching, to some extent but not completely, is also the cost of behaviour adaptation, which indicates the opportunity cost of not accepting the available options.

In addition to adapting to a new environment, the dACC has also been identified as playing a critical role in retaining the history of previous rewards (Kennerley et al., 2006; Wittmann et al., 2016), which could guide decision making based on one's previous experience. Similar to the role of the ACC, optimizes voluntary choice behaviour by learning the value of decisions in earlier experiences (Kennerley et al., 2006), as early learning theories suggest that the expected value of currently available options is influenced by the previous outcome of that option (Bayer & Glimcher, 2005).

Interestingly, the ACC has also been found to encode the value difference between the value of chosen and unchosen options, similar to the role of the vmPFC as mentioned in section 1.3. However, the value difference pattern signalled in the ACC exhibits an inverse pattern to that of the vmPFC. The ACC positively encodes the value of the unchosen option but negatively encodes the value of the chosen option (Kolling et al., 2012). Despite the vmPFC is involved in the valuation process, the search value is not encoded by the vmPFC but by the ACC during searching, which indicates the specific role of the ACC (Kolling et al., 2012). Despite the inverse value difference pattern in the ACC being observable across multiple-choice decision-

making tasks, the ACC displayed a default pattern in relation to the second chosen option from the first decision to the second decision, which should have been negatively encoded during the second decision. This indicates that the inverse value difference signal in the ACC is absent during subsequent binary-choice decision-making and lacks the same flexibility as the vmPFC, which can switch the pattern of value encoding between the first and second decisions (Boorman et al., 2013).

To sum up, the ACC is plays a crucial role in searching by encoding the value and cost of searching. It also encodes an inverse value difference signal between chosen and unchosen options during both binary and multiple-choice decision-making. Given that searching was one of the possible decisions in the designed decision-making task, the ACC was one of the candidate regions of interest in this study.

1.5 Intraparietal Sulcus

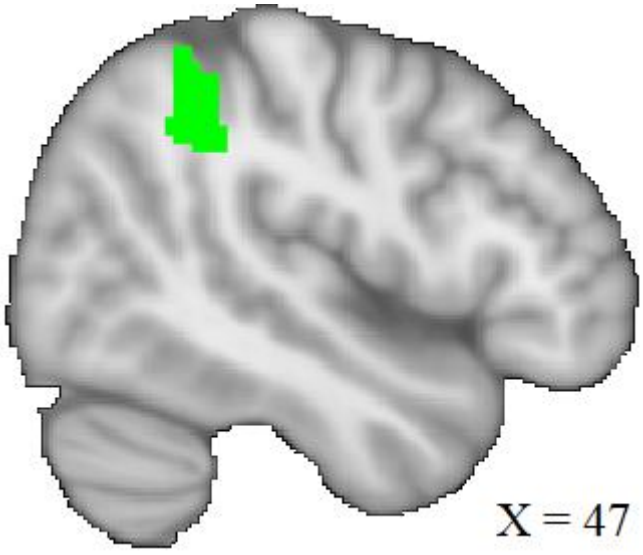

Figure 6. The Intraparietal Sulcus (IPS). The cluster of the IPS (green) was created from Mars et al. (2011).

The IPS was the third candidate region to be investigated in this study (Fig. 6). it is defined as the most prominent sulcus located on the lateral surface of the parietal lobe (Koutsarnakis et al., 2017), which includes Brodmann's areas 7, 19, 39, and 40 (Molko et al., 2003). It divides the posterior parietal cortex (PPC) into the superior parietal lobule (SPL) and the inferior parietal lobule (IPL) (Cabeza et al., 2008).

The role of the IPS have been investigated in some functional neuroimaging studies, and was found to be related to the risk-taking decision. For instance, it encodes the acceptance of risk (Huettel et al., 2006). Also, disrupting the IPS's activity reduces risk-taking decisions (Coutlee et al., 2016)

The lateral intraparietal area (LIP), one of the sub-regions of the IPS areas, has been widely studied in perceptual decision-making (Leathers & Olson, 2012; Platt & Glimcher, 1999; Shadlen & Newsome, 1996). In Shadlen and Newsome's (1996) study, monkeys were trained to perform a binary direction discrimination task. They found that LIP neurons carried predictive signals, which occurred several seconds prior to an eye movement indicating the monkeys' decisions. They therefore suggested that the predictive signals in LIP might constitute a neural correlate of decision formation in the central nervous system (CNS). Indeed, LIP neurons have been widely studied in visuospatial attention. For instance, the stronger activity in LIP neurons can describe the locus of attention (Goldberg et al., 2002). Also, previous studies suggested that saccadic eye movements and saccadic decisions are related to LIP neurons (Grefkes & Fink, 2005; Hanks et al., 2006; Marois & Todd, 2004; Shadlen & Newsome, 2001). Leathers and Olson (2012) found that LIP neurons can encode saccadic value, which could also mediate value-based decisions between saccades.

During value-based perceptual decision-making, Platt and Glimcher (1999) found that the activity of LIP neurons correlates with the subjective value of a particular response. Different from Shadlen and Newsome's (1996) study that the choices possess different reward amounts, the reward amounts are varied but could be expected from each possible eve-movement response. They showed that the activities of LIP neurons are modulated by the expected reward realized from the monkey's eye-movement responses.

LIP neurons have also been found to be related to information sampling and information gain (Foley et al., 2017; Gottlieb, 2018; Gottlieb et al., 2014; Gottlieb & Oudeyer, 2018; Horan et al., 2019). For instance, the accumulation of evidence about the environment and options is essential during value-based decision-making, and the extent to which the evidence is accumulated is important in that it guides us to make decisions (Gottlieb et al., 2014). When making decisions under uncertainty, gathering information is needed to reduce uncertainty. Decisions are made when the accumulation of evidence reaches one's internal boundary (Gold & Shadlen, 2007), similar to the perceptual decision-making task that decisions are made when sensory evidence has accumulated enough to reach the sensory threshold (Ratcliff et al., 2007). In Horan et al.'s (2019) study, two monkeys were trained to perform an information sampling task. The options were uncertain at first, where they could gather information before choosing between uncertain options. They showed that LIP neurons encode information gain and are more active in more informative trials.

Meanwhile, decision confidence, i.e. the extent to which people believe that they can make the best decision during decision-making, has been suggested to be encoded by the IPS in perceptual decision-making (Kiani & Shadlen, 2009). In

general, if we just have limited information about the future rewards, our decision confidence will be lower. Similar to the vmPFC, the IPS also encodes decision confidence (Hebscher & Gilboa, 2016; Shapiro & Grafton, 2020). This suggests that both IPS and vmPFC might share similar roles during various types of decision-making tasks.

To summarize, the LIP area plays a crucial role in various tasks such as visual searching, visuospatial attention, saccadic eye movement, perceptual decision-making, value-based decision-making, sensory evidence accumulation, information sampling, and information gain. These functional particularly relevant during information sampling, making the IPS an important region of interest.

1.6 The current study and research aim

In an uncertain environment, information sampling is required for making adaptive decisions. There are typically two types of information sampling: gathering more information about current options or searching for new options. Early literature have examined the neural mechanisms of deciding between selecting existing options and one of the two types of information sampling. However, there is a lack of a unified framework to describe the dynamics between considering these three decisions at the same time. This study aims to investigate the neural mechanisms of information sampling in multiple-choice decision-making.

To address this problem, the importance of value-based theories during information sampling are reviewed, including the valuation and value comparison processes. Three candidate brain regions were identified: the vmPFC which guides option selection; the IPS, which signals demand for information and information gain;

and the ACC, which is critical for searching for new options. The study used fMRI to examine the roles of these regions during the designed multiple-choice decision-making task. The details of the methods and results will be discussed in **Chapters 2, 3** and **4**.

Chapter 2: Behavioural hallmarks of information sampling in multiple-choice decision-making

Chapter highlights

1. This chapter aims to determine how participants made use of the information provided in a multiple-choice decision-making task to formulate decisions of accept, clarify and search.
2. The participants preferred to make more search than accept decisions.

2.1 Introduction

As mentioned in **Chapter 1**, there is a need for a comprehensive framework that incorporates the decisions involved in accepting currently available options, clarifying existing options, and searching for new options, particularly in the context of multiple-choice decision-making. A multiple-choice decision-making task was designed in this study. Since individuals might have different subjective preferences for various categories of stimuli (Bartra et al., 2013; Levy & Glimcher, 2012), to mitigate the impact of the stimuli categories, the stimuli used in value-based decision-making tasks are sometimes abstract and diverse. Researchers have developed a range of abstract stimuli used in the laboratories to test the underlying mechanisms of value-based decision-making. For instance, the stimuli could be bars (Hunt et al., 2013), rectangles (Strait et al., 2014) and pie charts (Yamada et al., 2018).

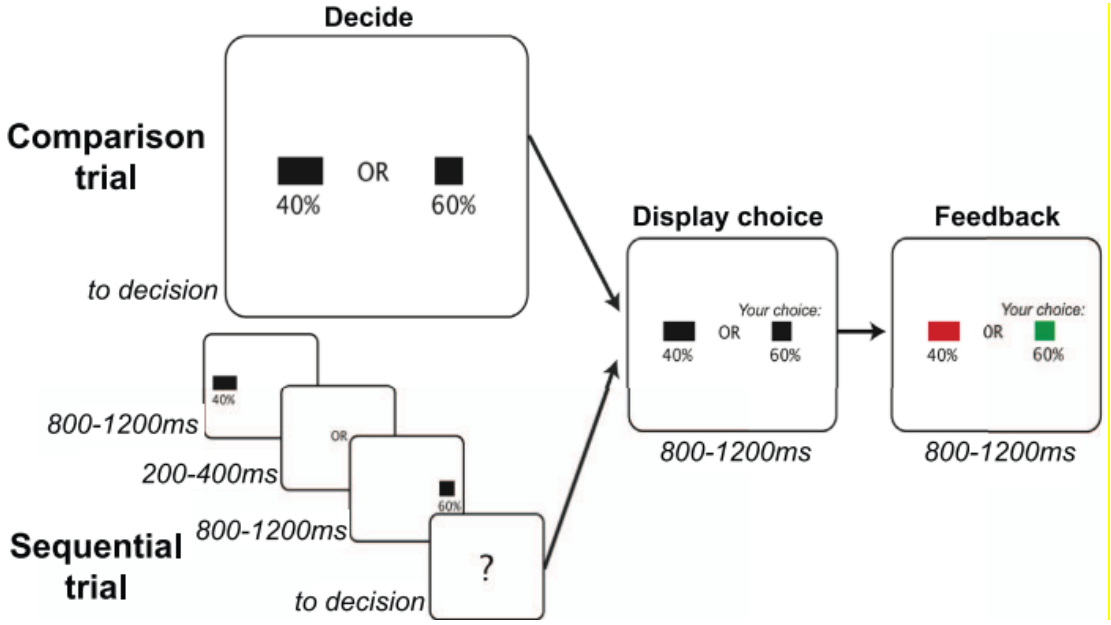

Figure 7. Stimuli used for studying the value-related signal in the human brain. People decided between two abstract stimuli which were associated with different reward magnitudes, with the reward probabilities displayed under the stimuli. The reward magnitudes were associated with the bar widths. Adapted from Hunt et al. (2013).

Employing abstracted stimuli can also enhance the generalizability of the results regardless of the categories of stimuli. Also, stimuli are quantifiable. For instance, reward magnitude, which is a kind of value information can be reflected by simply displaying its value (Guo et al., 2017), the coloured proportion in the abstract stimuli (Strait et al., 2014; Yamada et al., 2018), and their sizes (Hunt et al., 2013). Figure 7 shows an example study that adopted abstract stimuli to investigate the value-related processes in the human brain, which the processes were then visualized by neural signals in the brain (Hunt et al., 2013). Since the main problem of this study concerns information sampling, the information could be related to different objects. The designed decision-making task in this study therefore also adopted abstract

stimuli to reduce the subjective preference for certain objects to increase the generalizability (i.e., dials, Fig. 8).

In this chapter, I will first demonstrate how the participants valued different information provided in a decision-making task to formulate different decisions (i.e., accept, clarify and search). I also designed three decision values (i.e., the accept, clarify and search values) to specify how the participants decided between the three possible decisions in the task. These decision values were then correlated with brain activities to investigate the neural mechanisms, which will be discussed in Chapter 3.

2.2 Methods

2.2.1 Participants

Twenty-six healthy right-handed adults with normal or corrected-to-normal vision and without current, or a history of, neurological and psychiatric problems were recruited by convenience sampling. Written informed consent was given by each participant before the experiment. The Human Subjects Ethics Committee of The Hong Kong Polytechnic University approved this study.

2.2.2 Decision-making task

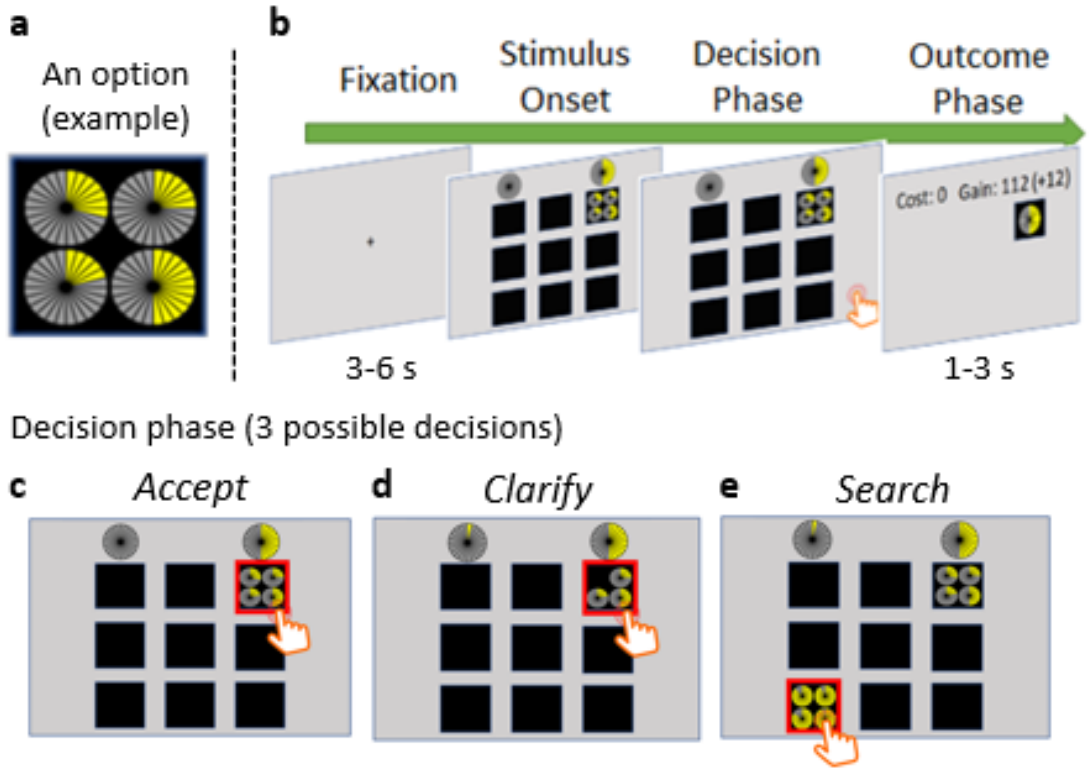

Figure 8. A multiple decision-making task. ***a*** *Each option had four dials (top-left panel), which indicated the number of points that could be potentially obtained (coloured sectors). The number of points that could be actually obtained by each option was related to only one of its dials. Therefore, options that had more varied dials would be more uncertain.* ***b*** *There was a fixation cross at the centre of the screen at the beginning of each trial (3-6 s). An option would randomly appear at one of the nine positions (black boxes). The participants needed to make one of the three possible decisions (Decision Phase). The first decision (i.e., clarify) could reduce the uncertainty of a selected option as one of its dials would be randomly removed after each clarify decision. The second decision (i.e., search) could reveal a new option from one of the black boxes. The third decision (i.e., accept) could gain the actual points of the option, and the amount would be revealed and delivered to the participants (Outcome Phase). Each clarify or search decision cost a point. A dial at*

the top left-hand corner of the screen recorded the cumulated cost in a single trial. The cost would be charged at the end of each trial. Another dial at the top right-hand corner of the screen signalled the average point among all (hidden and revealed) options in a current trial.

The multiple-choice decision-making task was adopted to test how the participants decided between accepting existing options and information sampling. At the beginning of each trial, the participants were offered an option (Fig. 8a). Each option in this task possessed four dials, while the proportion of the coloured area of each dial indicated the number of points that could be potentially obtained. There were three possible decisions (i.e., accept, clarify and search) that the participants could make. First, accepting a current option would pseudo-randomly obtain the points of one of the dials (Outcome Phase, Fig. 8b & 8c). The participants were told that all dials in all options shared the same probability. Second, clarifying a current option would remove one of the dials pseudo-randomly at the expense of one game point to reduce the uncertainty of the option (Fig. 8d). For any given option, the participants could clarify it up to three times. Third, searching for an alternative option at the expense of one game point, in which a new option with four dials would appear (Fig. 8e). Since there was a maximum of nine options, the participants could search for up to eight times. The average game point of all options (hidden and revealed) in the same trial was displayed at the top-right of the screen, such that participants could determine whether to search or not based on this average and the options that were offered. Participants were asked to obtain as many points as possible in 100 trials.

2.2.3 Statistical analysis

To describe how participants made use of the information to decide between decisions of accept, clarify and search, I defined three decision values (i.e., the accept value, clarify value and search value). Since the cost (i.e., the cumulative cost in the decision-making task) has been suggested to be essential in information sampling, it was accompanied by these three decision values and entered into a General Linear Model 1 (GLM1). This could help us to understand how each of the three decisions were evaluated by the participants in a multinomial logistic regression analysis as follows:

GLM1:

$$y = \beta_0 + \beta_1 Value_{Accept} + \beta_2 Value_{Clarify} + \beta_3 Value_{Search} + \beta_4 Cost$$

where y is the choice to *accept(0)*, *clarify(1)* or *search(2)*, while $Value_{Accept}$, $Value_{Clarify}$ and $Value_{Search}$ are decision values associated with decisions of accept, clarify and search, and $Cost$ is the cumulated cost. This multinomial logistic regression analysis was adopted using MATLAB (mnrfit) to predict whether the participants decided between decisions of accept, clarify or search. All regressors were normalized to ensure the commensurability of the regression coefficients. Since participants might have different motives to accept, clarify and search, 47 models adopting different operational definitions of the decision values were compared. Thus, the decision values with the best predictive powers could be defined.

Table 1. Type of the accept, clarify and search value adopted by models

Model	Accept Value	Clarify Value	Search Value
1	Type1	Type1	Type1
2	Type1	Type3	Type1
3	Type1	Type1	Type2
4	Type1	Type3	Type2
5	Type2	Type1	Type2
6	Type2	Type10	Type2
7	Type3	Type3	Type2
8	Type3	Type11	Type2
9	Type1	Type10	Type2
10	Type1	Type11	Type2
11	Type1	Type1	Type3
12	Type1	Type3	Type3
13	Type1	Type10	Type3
14	Type1	Type11	Type3
15	Type3	Type10	Type3
16	Type2	Type11	Type3
17	Type1	Type4	Type2
18	Type1	Type5	Type2
19	Type1	Type6	Type2
20	Type1	Type7	Type2
21	Type1	Type7	Type4
22	Type1	Type6	Type4
23	Type1	Type12	Type4
24	Type1	Type13	Type4
25	Type1	Type14	Type4
26	Type2	Type14	Type4
27	Type3	Type7	Type4
28	Type2	Type13	Type4
29	Type1	Type7	Type4
30	Type1	Type6	Type5
31	Type1	Type7	Type5
32	Type1	Type14	Type5
33	Type1	Type12	Type5
34	Type1	Type13	Type5
35	Type3	Type12	Type5
36	Type3	Type13	Type5
37	Type1	Type2	Type2
38	Type1	Type7	Type1
39	Type1	Type6	Type1
40	Type1	Type9	Type1
41	Type1	Type8	Type1
42	Type1	Type12	Type1
43	Type1	Type12	Type2
44	Type1	Type12	Type2
45	Type1	Type13	Type1
46	Type1	Type13	Type2
47	Type1	Type13	Type4

First, I formulated three types of the accept value as follows:

$$Accept\ Value_{\ (1)} = Value_{\ (the\ best\ option)}$$

$$Accept\ Value_{\ (2)} = \frac{Value_{\ (the\ best\ option)}}{Variance_{\ (the\ best\ option)}}$$

$$Accept\ Value_{\ (3)} = \frac{Value_{\ (the\ best\ option)}}{StandardDeviation_{\ (the\ best\ option)}}$$

Since it could be expected that the participants would prefer to accept the option with the greatest average value, the first type of the accept value (*Accept Value $_{(1)}$*) was formulated as the average value of that option (i.e., the best option). I also wanted to investigate if the uncertainty of the best option would discount the value, so I used the variance and standard deviation to indicate the uncertainty. The second and third types of the accept value were similar to the *Accept Value $_{(1)}$* but divided by the variance of the best option (*Accept Value $_{(2)}$*) and the standard deviation of the best option (*Accept Value $_{(3)}$*) respectively.

Second, I formulated 14 types of the clarify value as follows:

Clarify Value $_{(1)}$ = $Variance_{\ (the\ best\ option)}$

Clarify Value $_{(2)}$ = $Variance_{\ (clarified\ option)}$

Clarify Value $_{(3)}$ = $StandardDeviation_{\ (clarified\ option)}$

Clarify Value $_{(4)}$ = $maxValue_{\ (clarifed\ option)} - minValue_{\ (clarified\ option)}$

Clarify Value $_{(5)}$ = $medianValue_{\ (clarified\ option)}$

Clarify Value $_{(6)}$ = $maxVariance_{\ (option)}$

Clarify Value $_{(7)}$ = $maxStandardDeviation_{\ (option)}$

Clarify Value $_{(8)} = max(maxValue_{(option)} - minValue_{(option)})$

Clarify Value $_{(9)} = \max(\text{medianValue})_{(\text{option})}$

Clarify Value $_{(10)} = Value_{(clarified\ option)} * Variance_{(clarified\ option)}$

Clarify Value $_{(11)} = Value_{(clarified\ option)} * StandardDeviation_{(clarified\ option)}$

Clarify Value $_{(12)} = max(Value_{(option)} * Variance_{(option)})$

Clarify Value $_{(13)} = max(Value_{(option)} * StandardDeviation_{(option)})$

Clarify Value $_{(14)} = max(Value_{(option)} * (maxValue_{(option)} - minValue_{(option)}))$

Since an option with a larger uncertainty is worthy of being clarified, I first focused on the best option. The first type of clarify value was defined as the variance of the best option (*Clarify Value* $_{(1)}$). I then focused on the option that was selected to be clarified. The second and third type of the clarify value were formulated as the variance (*Clarify Value* $_{(2)}$) and the standard deviation of the clarified option (*Clarify Value* $_{(3)}$) respectively. Other information that indicated a larger uncertainty was the value difference between the dials within an option. Therefore, I formulated the fourth type of the clarify value based on the value range of the clarified option (*Clarify Value* $_{(4)}$). Meanwhile, the best and worst results of a clarify decision were to remove a dial with the smallest and greatest value respectively. The fifth type of the clarify value was formulated as the median value of the clarified option, implying that the results of clarify decisions were averaged (*Clarify Value* $_{(5)}$).

Apart from the clarified option, I also focused on the uncertainty of all revealed options. The sixth, seventh, eighth and ninth types of the clarify value were formulated as the greatest variance (*Clarify Value* $_{(6)}$), the greatest standard deviation

(*Clarify Value* $_{(7)}$), the greatest value range (*Clarify Value* $_{(8)}$), and the greatest median value (*Clarify Value* $_{(9)}$) among all revealed options respectively.

I also focused on both value and uncertainty. This suggested that an option that was worth being clarified should have a greater average value and was also largely uncertain. The tenth and eleventh types of the clarify value were formulated as the product between the value and the variance of the clarified option (*Clarify Value* $_{(10)}$), and the standard deviation of the clarified option (*Clarify Value* $_{(11)}$).

I also focused on all revealed options. The twelfth, thirteenth and fourteenth types of the clarify value were formulated as the greatest product between the value and the variance (*Clarify Value* $_{(12)}$), the greatest product between the value and the standard deviation (*Clarify Value* $_{(13)}$), and the greatest product of the value and the range of the value (*Clarify Value* $_{(14)}$) among all revealed options respectively.

Third, I formulated five types of the search value as follows:

Search Value $_{(1)} = \overline{Value}_{(all\ options)}$

Search Value $_{(2)} = \overline{Value}_{(all\ existing\ options)}$

Search Value $_{(3)} = Value_{(new\ option)}$

Search Value $_{(4)} = \overline{Value}_{(all\ options)} - \overline{Value}_{(all\ existing\ options)}$

Search Value $_{(5)} = \overline{Value}_{(all\ options)} - Value_{(the\ best\ option)}$

Since the value of the environment was one of the drives to search, the first type of the search value was formulated as the average value of all hidden and revealed options (*Search Value* $_{(1)}$). The second type of the search value was

formulated as the average value among all revealed options (*Search Value* $_{(2)}$), as a smaller average value would drive the search for better alternatives.

Meanwhile, since searching has been suggested to be an adaption behaviour for a new environment (Behrens et al., 2007; Quilodran et al., 2008; Wessel et al., 2012), I also focused on searching when there was a new option. The third type of the search value was formulated as the value of the new option (*Search Value* $_{(3)}$). The new option could be the first option that appeared at the beginning of each trial, i.e. the most recent searched or clarified option.

I also investigated the value difference between existing options and the environment that might drive a search. The fourth and fifth types of the search value were formulated as the average value of all hidden and revealed options minus the average value of all revealed options (*Search Value* $_{(4)}$), and the average value of all options minus the average value of the best option (*Search Value* $_{(5)}$).

To select the model with the greatest predictive power, the Bayesian information criterion (Schwarz, 1978) was used. Data from all trials were used to compute the BIC value among the participants for each model. The BIC values obtained from each participant were averaged and then compared between models. The model with the lowest average BIC indicated that the model had the best fit to the data compared with other models. The decision values defined in the best fit model would be used in the following analyses.

2.3 Results

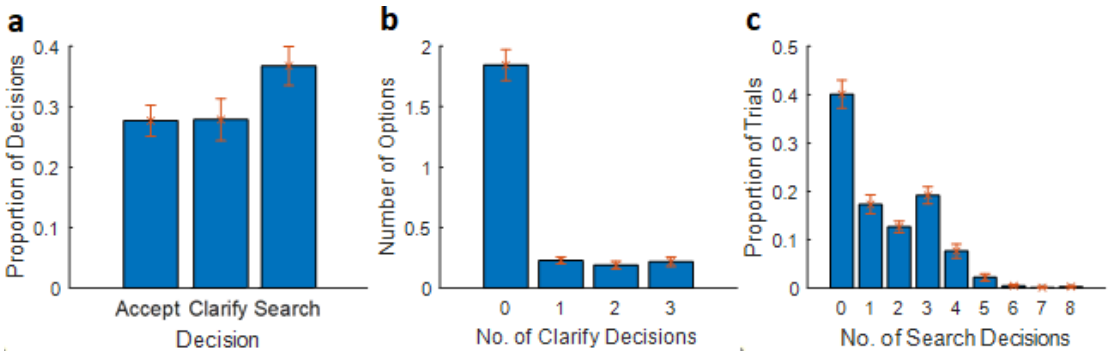

Figure 9. Behavioural analyses. ***a*** *Task performance. The proportion of the three types of decisions made by the participants.* ***b*** *The preference of the number of clarify decisions across trials.* ***c*** *The average number of search decisions made by the participants.*

Figure 9 provides an overview of the decisions made by the participants throughout the multiple-choice decision-making task. First, the participants' decisions were 29.99% accept decisions, 30.19% clarify decisions and 39.82% search decisions (Fig. 9a). Second, I further analyzed how frequently the participants made clarify decisions. I found that there was an average 23 option that was clarified once, 19 option that was clarified twice, and 22 option that was clarified three times in 100 trials (Fig. 9b). Third, I also analyzed how frequently the participants made search decisions. I found that the participants searched for a new option at least once in 59.92% of all trials (i.e. made 0 search decisions in 40.08% of trials) (Fig. 9b). Interestingly, within the trials that the participants made at least one search decision, even though it would cost a point each time, the participants preferred to search for three times as the most (19.17%), but not once (17.29%) or twice (12.67%; Fig. 9c).

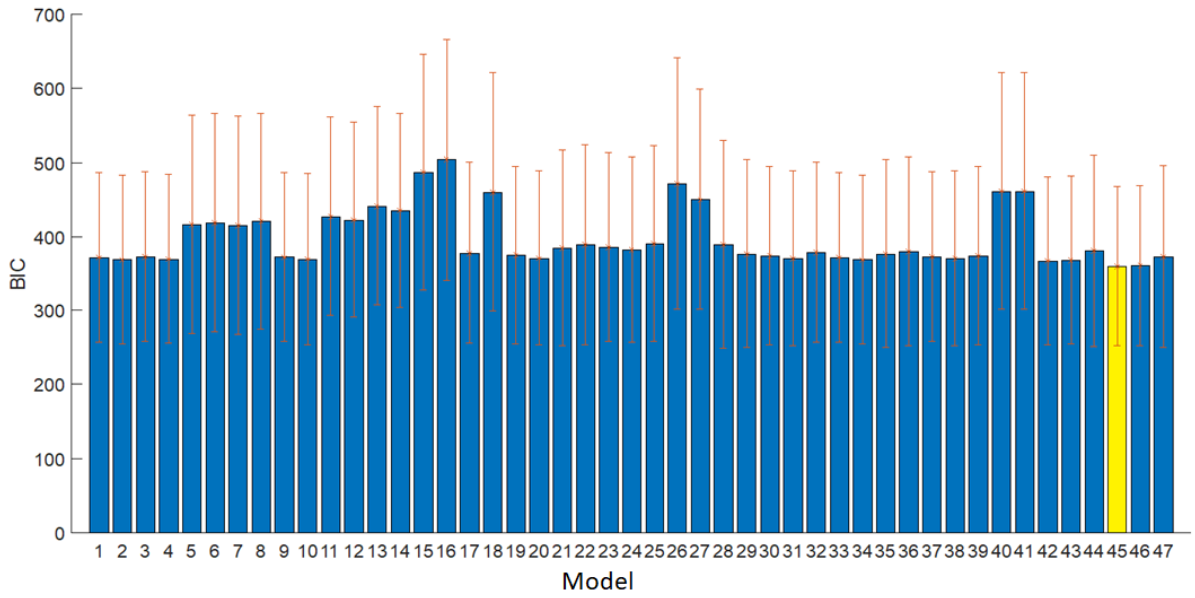

Figure 10. Model comparison based on the Bayesian Information Criterion (Schwarz, 1978). The average BIC value was computed among the participants for each model and was compared between 47 models. The yellow bar indicates the best model with the lowest BIC value. Error bars represent means±s.e.m.

Next, I aimed to identify the parameters that best described the participants' decisions. To achieve this, I fitted the participants' choice data using variants of GLM1, with each variant involving different definitions of the values of the accept, clarify and search decisions. The details of the method for defining the decision values were described in section 2.2.3. Model comparison between each average BIC value from each model was conducted (Fig. 10). For the model with the lowest average BIC value (the yellow bar, the average BIC value=360.05, Fig. 10), the accept value was defined as the average value of the best option, which possessed the largest value among all revealed options; the clarify value was defined as the greater product between the option's average value and its standard deviation, which could ensure that an option with a large value but a small standard deviation, or with a large standard deviation but a small value was not worth being clarified; the search value

was defined as the average value among all hidden and revealed options, which was the same as the value displayed at the top-right of the screen.

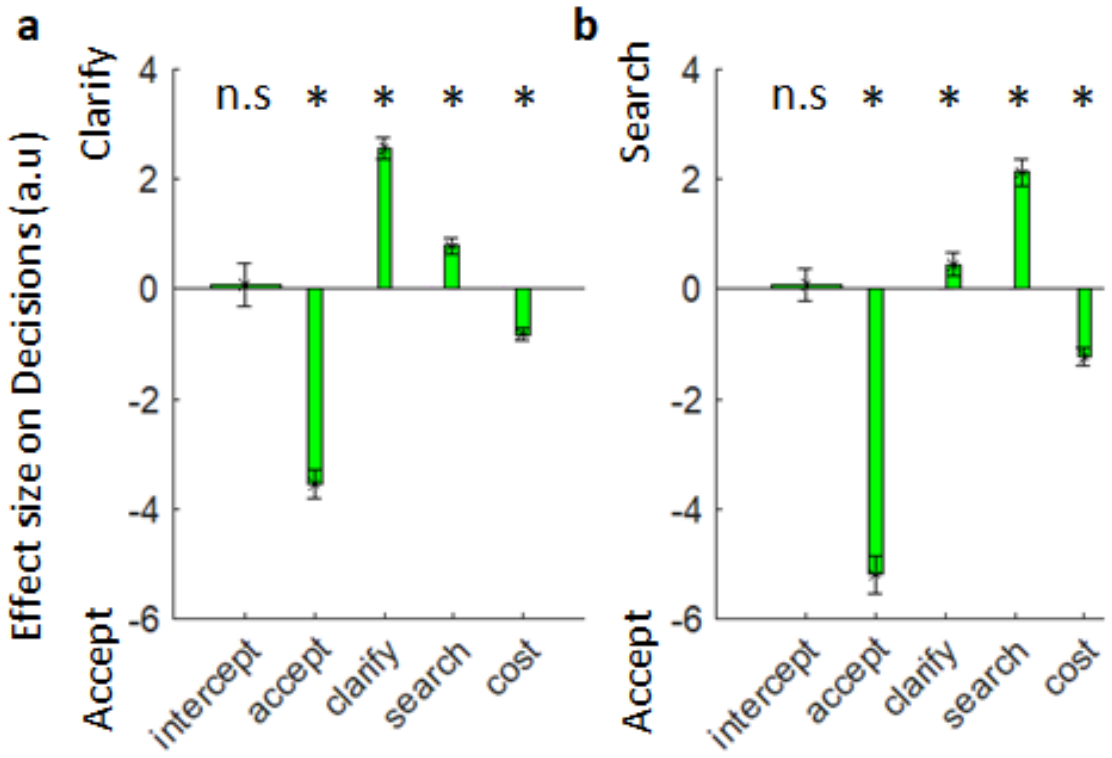

Figure 11. A multinomial logistic regression. ***a*** *The effects of accept, clarify and search values on the proportion between clarify and accept decisions,* ***b*** *search and accept decisions as well. n.s. denotes* $p > .05$. * *denotes* $p < .05$. *Error bars represent means±s.e.m.*

The results of the multinomial logistic regression analysis for the best model are displayed in Figure 11, which helps us understand how the participants made use of the information provided in the decision-making task to decide between different decisions. The choice ratio between clarify and accept decisions was positively associated with the clarify value (β=2.558, $t(23)$=12.920, P<0.001, Fig. 11a), negatively associated with the accept value (β=-3.540, $t(23)$=-13.115., P<0.001, Fig. 11a), and negatively associated with the cumulated cost (β=-0.819, $t(23)$=-6.597, P<0.001, Fig. 11a).

Surprisingly, the choice ratio between clarify and accept decisions was positively associated with the seemingly irrelevant search value (β=0.784, $t(23)$=5.282, P<0.001, Fig. 11a), which was supposedly not relevant to that choice context, which the search value was not supposed to be related to clarify decisions. On the other hand, the choice ratio between search and accept decisions was positively associated with the search value (β=2.125, $t(23)$=9.092, P<0.001, Fig. 11b), negatively associated with the accept value (β=-5.193, $t(23)$=-15.150, P<0.001, Fig. 11b), and negatively associated with the cumulated cost (β=-1.222, $t(23)$=-7.832, P<0.001, Fig. 11b). Similar to the results of the irrelevant search value on the choice ratio between clarify and accept decisions, a surprising result was also found that the choice ratio between search and accept choice was positively associated with the clarify value (β=0.450, $t(23)$=2.088, P=0.0481, Fig. 11b), because the clarify value was supposedly not relevant to that choice context. Critically, the results suggest that the participants were also more inclined to search or clarify when they were dissatisfied with the current offers.

2.4 Conclusion

In this chapter, I presented the designed multiple-choice decision-making task and provided an overview of the behavioural results. I adopted a multinomial logistic regression analysis to understand how the participants made use of the information to make decisions, which help to define the most predictive decision values for each decision through model comparisons. The results identified that the accept, clarify, and search values had the most predictive power for decisions of accept, clarify, and search, respectively. These well-defined decision values also then correlated with brain activities to investigate the neural mechanisms underlying different decisions through a series of whole-brain analyses, ROI time-course analyses with specific regions-of-

interest (ROIs), and artificial neural networks, which will be discussed in the following chapters.

Chapter 3: Neural mechanisms underlying information sampling during multiple-choice decision-making

Chapter highlights

1. This chapter aims to test the neural mechanisms underlying accept, clarify and search decisions.
2. The vmPFC, IPS and ACC were found to play a critical role in decisions of accept, clarify and search, respectively.
3. Value difference signal was also found in the vmPFC in the multiple-choice decision-making task.
4. The IPS signalled both the demand for information and gain in information.
5. The ACC signalled the competition between search and accept decisions first, followed by search and clarify decisions.

3.1 Introduction

In the last chapter, I illustrated how the participants made use of the information to decide between decisions of accept, clarify and search. In this chapter, the analyses mainly focus on neural mechanisms of accept, clarify and search decisions. The well-defined decision values would be adopted to be correlated with the fMRI data to examine the roles of specific brain regions during these decisions in multiple-choice decision-making. This chapter presents the methods and results of the fMRI data.

3.2 Methods

3.2.1 Participants

The participants were the same as mentioned in section 2.2.1. Particularly in this chapter, those participants who passed the safety screening of fMRI scanning were invited to participate in the experimental task under fMRI scanning. Two of them were excluded from the data analyses due to exaggerated movement during fMRI scanning.

3.2.2 Decision-making task

The decision-making task was the same as mentioned in section 3.2.2.

3.2.3 Neuroimaging data acquisition and preprocessing

Neuroimaging data were acquired on a Siemens MAGNETOM Prisma 3-T MRI scanner. FMRI data were acquired with $2 \times 2 \times 2$ mm^3 voxel resolution, TR=2000 ms, TE=30 ms, flip angle=75°, slice angle=15°, and multi-band acceleration factor=3. Field maps were acquired with echo sequence: $2 \times 2 \times 2$ mm^3 voxel resolution, TR=753 ms, TE1=5.16 ms, and TE2=7.62 ms. T1-weighted structural images were acquired with $1 \times 1 \times 1$ mm^3 voxel resolution, $256 \times 256 \times 208$ grid, TR=1900 ms, TE=3.37 ms, TI=900 ms, iPAT acceleration factor PE=2, and iPAT acceleration factor 3D=1.

FMRIB's Software Library (FSL) was used for preprocessing of fMRI data (Smith et al., 2004). The procedures for image preprocessing included motion correction (Jenkinson et al., 2002), brain extraction (Smith, 2002), field map correction for distorted signals (Jenkinson, 2003), and Gaussian spatial smoothing using high-pass temporal filtering (3 dB cut-off of 100s) with full width at half

maximum (FWHM) sizes of 5 mm. FMRI data were then registered to the high-resolution structural images for each participant and normalized into the standard Montreal Neurological Institute (MNI) space (Jenkinson & Smith, 2001).

3.2.4 Statistical Analysis

To examine the neural mechanisms underlying accept, clarify and search decisions, the accept value, clarify value, search value and cumulative cost were entered as regressors into the whole-brain analysis to see if they could be identified in the specific brain region. A univariate GLM approach for the statistical analysis of the whole-brain analyses was conducted using FEAT (Beckmann et al., 2003; Woolrich et al., 2004). The main effect images were all cluster-corrected results with the voxel inclusion threshold of z=3.1 and the threshold of cluster significance=0.05 (*p*-value). After specific brain regions were identified, the time-courses from the identified brain regions were extracted according to the defined regions of interest (ROIs) in existing literature for ROI time-course analyses. The activities of the ROIs were then correlated with the decision values to visualize the signals. This analysis contrasted the regression weights of the decision values to brain activity changes over time and identified the peak signal during decision-making. A leave-one-subject-out procedure was used to find the peak time (within a window of 0 to 15 s/20 s) for all subjects excluding the left-out one. This was repeated 23 times to ensure that each participant was left out once, and the results were averaged. Peak window selection used full width at half maximum, in which the window was defined by the two-time points that were equal to half of their maximum value (i.e., the regression weight). The identified peak was adopted for individual analyses, to identify the correlation between the beta peak BOLD signals and the proportion of decisions. All ROI time-course analyses were done in MATLAB.

3.3 Results

3.3.1 VmPFC and accept decision

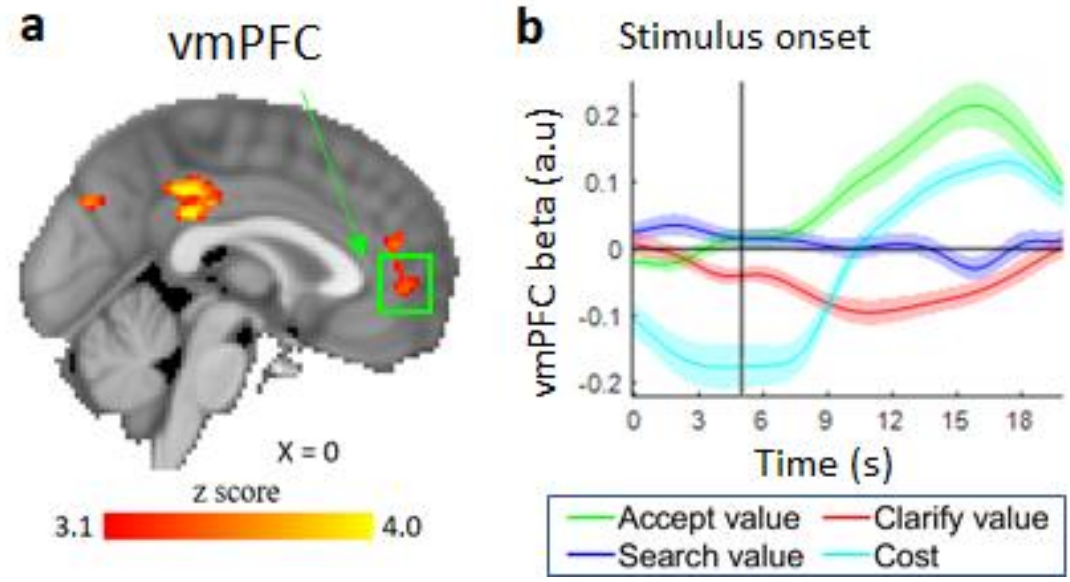

Figure 12. Analyses of the accept decision. ***a*** *Whole-brain analysis. The vmPFC activity was identified to be associated with the accept value (red region within the green box). I extracted the identified region as ROI for the ROI time-course analyses.* ***b*** *A ROI time-course analysis. The three decision values and the cumulative cost estimated by the vmPFC activity throughout the whole decision-making task across time. The vertical line in the ROI time-course analysis signalled the stimuli onset at 5 s, and leave-one-out peak selection was adopted for the ROI time-course analysis.*

I first focused on the neural mechanisms underlying the accept decision. The results of the whole-brain analysis found that several regions were positively related to the accept value (i.e., the average value of the best option) ($P < 0.05$, cluster-level corrected [$z > 3.1$]; Fig. 12a), such as the vmPFC (all significant regions that were identified to be related to the accept value in the whole-brain analysis are shown in Table 2).

Table 2. Identified regions from whole brain analyses for regressors-of-interest					
Accept Value					
Brodmann's areas	**Common names**	**MNI coordinates**	**Max Z-score**	**P-value**	**# voxels**
10	Ventral medial prefrontal cortex				
	-Left	(-36 46 -2)	4.84	1.6e-05	387
	-Right	(40 48 -10)	3.74	0.0439	113
9	Superior frontal cortex				
	-Right	(52 38 26)	4.09	0.0189	137
46	Medial prefrontal cortex				
	-Right	(42 34 12)	4.34	0.0296	124
32	Pregenual anterior cingulate cortex				
	-Left	(-4 44 20)	4.20	0.0051	177
39	Angular gyrus			2.25e-	
	-Left	(-52 -62 38)	5.42	05	373
23	Posterior cingulate cortex				
	-Right	(0 -36 30)	4.18	0.0003	268
	Caudate				
	-Right	(12 14 -4)	4.68	0.0144	145
21	Medial temporal gyrus				
	-Left	(-60 -26 -14)	4.31	0.011	153
8	Frontal eye field				
	-Left	(-38 26 44)	4.60	0.0276	126
18	Secondary visual cortex			2.33e-09	
	-Left	(20 -98 -2)	5.66	7.58e-	800
	-Right	(24 -86 0)	5.29	05	325
	-Left	(-6 -78 36)	4.25	0.0249	129

Previous studies have commonly suggested that the vmPFC is related to the value of the chosen option, while it is usually the best option (Chau et al., 2014; Hunt et al., 2012; Strait et al., 2014). I therefore extracted the BOLD time course of the identified vmPFC to run a ROI time-course analysis as an alternative approach to visualize the accept signal in the vmPFC. The accept value, clarify value, search value and cumulative cost were entered as regressors into the ROI time-course analysis to examine the association with the vmPFC BOLD activity across time. A positive accept signal was found (green), and the peak vmPFC BOLD β weights were 10.9 to 19.8 s (leave-one-out peak selection, $t(23)$ =6.345, P<0.001, Fig. 12b). In other words, the vmPFC activity was stronger while the accept value was greater.

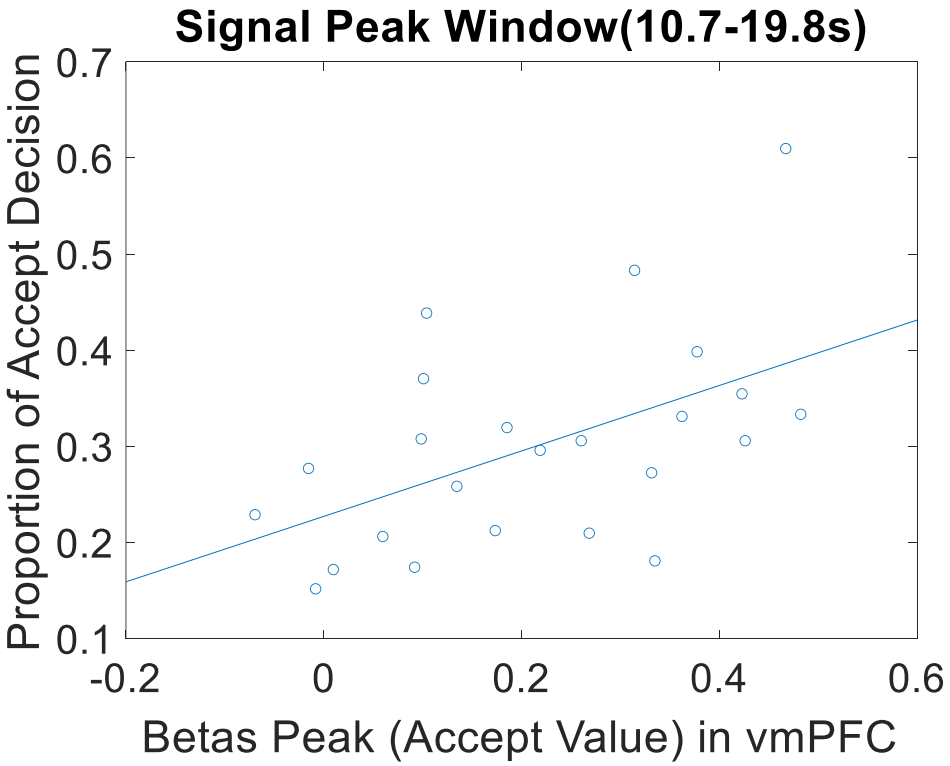

Figure 13. Individual analysis of the association between the peak of the vmPFC signal and the proportion of accept decisions across subjects (N=24)

The peak of the vmPFC signal from each participant was then extracted to run a between-subject analysis. The results showed that the size of the participants' peak signal was positively correlated with the proportion of accept decisions made by the participants in the task (r=.519, P=0.009. Fig. 13). In other words, relatively more accept decisions and less clarify or search decisions were made by the participants when they had greater accept signals in their vmPFC. I further looked at the role of the vmPFC during the decision-making task.

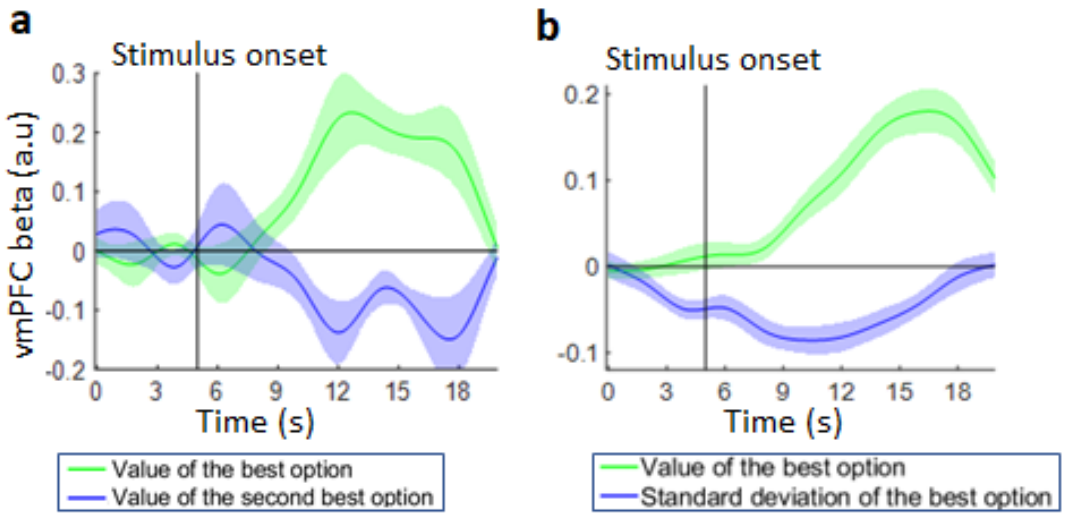

Figure 14. ***a*** *Value difference signal was found in the vmPFC.* ***b*** *An uncertainty aversion pattern was found in the vmPFC(blue). The vertical lines in all ROI time-course analyses signalled the stimuli onset at 5 s, and leave-one-out peak selection was adopted for all ROI time-course analyses.*

Since previous findings have suggested that the vmPFC encodes the value difference signal between chosen and unchosen options (Jocham et al., 2012; Strait et al., 2014), the average value of the best option and second best option were entered into the ROI time-course analysis as regressors to see if the value difference signal also occurred in this study. The results showed a positive best value signal (green) at the peak vmPFC BOLD β weights during 10.3 to 16.1 s ($t(23)$ =5.018, P<0.001, Fig. 14a)

and a negative second-best value signal (blue) at the peak vmPFC BOLD β weights during 10.4 to 14.1 s ($t(23)$ =-2.702, P=0.013, Fig. 14a), indicating that a prominent value difference (the average value of the best option minus second-best option) signal occurred in the vmPFC. Surprisingly, the analysis also found a negative clarify signal (red) in the ROI time-course analysis at the peak vmPFC BOLD β weights during 7 to 17.3 s ($t(23)$ =-4.755, P<0.001, Fig. 12b). Since the clarify value was defined by the product between the value and the standard deviation (i.e., uncertainty) of the option, the value information of the clarify value might share similarity with the accept value (r=.916, P<.001). I further analyzed if this negative clarify signal might be contributed by the second component of the clarify value (i.e., the standard deviation or the uncertainty of the option) and negatively associated with the vmPFC BOLD activity. I therefore ran a subsequent analysis for the vmPFC. A negative uncertainty signal was found in the vmPFC (blue) at the peak vmPFC BOLD β weights during 5.8 to 16.2 s ($t(23)$ =-5.094, P<0.001, Fig. 14b). The result might be suggested by previous findings that people discount the value of an option based on its uncertainty due to the risk aversion nature of humans. Also, the vmPFC has been suggested to be related to decision confidence (Hebscher & Gilboa, 2016; Shapiro & Grafton, 2020), so the participants would have less confidence when deciding to accept an option when it is largely uncertain as the outcome is more unpredictable as well.

3.3.2 IPS and clarify decision

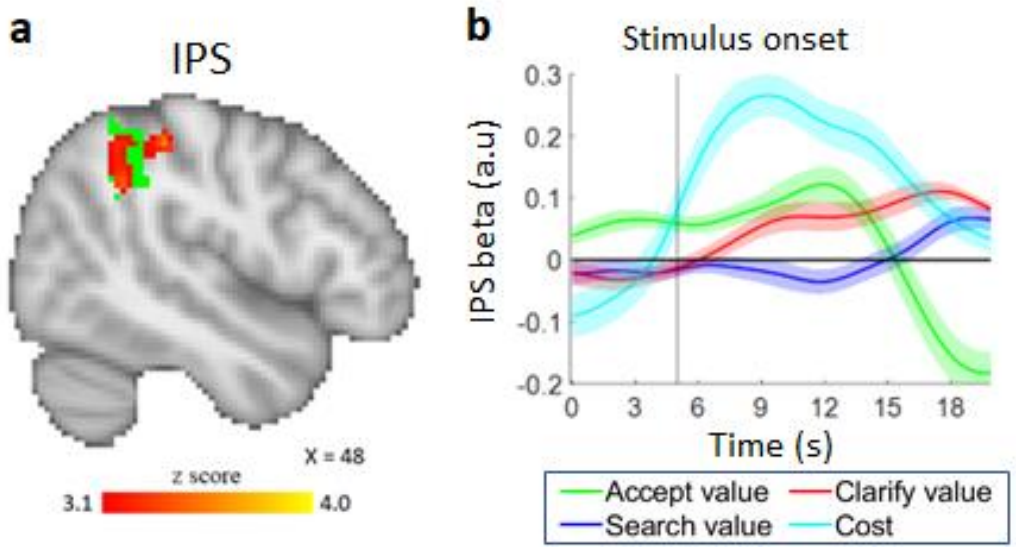

Figure 15. Analyses of the clarify decision. ***a*** *Whole-brain analysis. The IPS activity was identified to be positively correlated with the clarify value (red). The region (green) was defined as the ROI for the time-course analyses with coordinates taken from Mars et al. (2011).* ***b*** *A ROI time-course analysis. The three decision values and the cumulative cost were estimated by the IPS activity throughout the whole decision-making task across time. The vertical lines in the ROI time-course analysis signalled the stimuli onset at 5 s, and leave-one-out peak selection was adopted for the ROI time-course analysis.*

Next, I focused on the neural mechanisms underlying the clarify decision. The clarify value was found to be positively related to several regions which were identified from the results of the whole-brain analysis ($p < .05$, cluster-level corrected [$z > 3.1$]; Fig. 15a), including the IPS (all significant regions that were identified to be related to the clarify value in the whole-brain analysis are shown in Table 3).

Table 3. Identified regions from whole-brain analyses for regressors-of-interest					
Clarify Value					
Brodmann's areas	**Common names**	**MNI coordinates**	**Max Z-score**	**P-value**	**# voxels**
40	Intra-parietal sulcus			2.50e-	
	-Left	(-46 -36 44)	8.60	09	802
	-Right	(48 -32 48)	2.11	0.0076	165
7	Superior parietal gyrus				
	-Right	(6 -64 48)	1.77	0.017	141
4,6	Superior frontal gyrus	(-24 20 56)	2.52	0.0030	195
45	Inferior frontal gyrus				
	-Left	(-28 30 2)	3.57	0.0002	279
10	Ventral medial prefrontal cortex				
	-Left	(-30 58 10)	1.47	0.0338	121
11	Orbital frontal cortex	(28 30 0)	2.22	0.0059	173
6	Supplementary motor area			6.94e-	
	-Right	(22 14 56)	8.16	09	749
8	Frontal eye field				
	-Right	(8 38 32)	3.43	0.0003	267
	Cerebellum	(-34 -66 -26)	3.53	0.0002	276

Since the IPS has been suggested to be related to information gain and it guides the active information search behaviour (Foley et al., 2017; Horan et al., 2019), I also extracted the time course from the IPS with the coordinates shown in green (Fig. 15a) to run a ROI time-course analysis as an alternative approach to visualize the clarify signal in the IPS (Mars et al., 2011). The accept value, clarify value, search value and cumulative cost were entered as regressors into the ROI time-course analysis to examine the association with the IPS BOLD activity across time. Similar to the results of the vmPFC time-course analysis that a positive accept signal (green) was also found at the peak IPS BOLD β weights during 6.8 to 14.4 s ($t(23)$ =3.671, P<0.001,

Fig. 15b), these results were consistent with previous findings suggesting that the IPS would engage in the valuation process during perceptual decision-making tasks (Platt & Glimcher, 1999; Shadlen & Newsome, 1996, 2001).

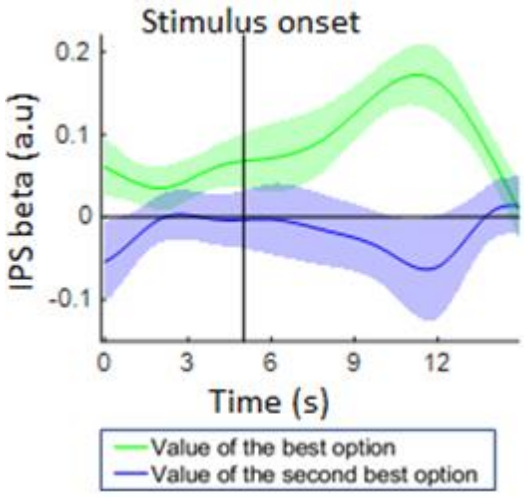

Figure 16. Subsequent ROI time-course analysis. The IPS could only signal the value of the best option but not the value difference between the chosen and unchosen options. The vertical lines in the ROI time-course analysis signalled the stimuli onset at 5 s, and leave-one-out peak selection was adopted for the ROI time-course analysis.

I then further analyzed if a value difference signal could also be found in the IPS. However, the result only found the best value signal ($t(23)$=4.773, P<0.001, Fig. 16) but the second-best value signal was absent (n.s.), indicating that the value difference signal was not found in the IPS. Critically, the results of the ROI time-course analysis also found a positive clarify signal (red) at the peak IPS BOLD β weights during 12.3 to 20.0 s ($t(23)$ =-5.908, P<0.001, Fig. 15b).

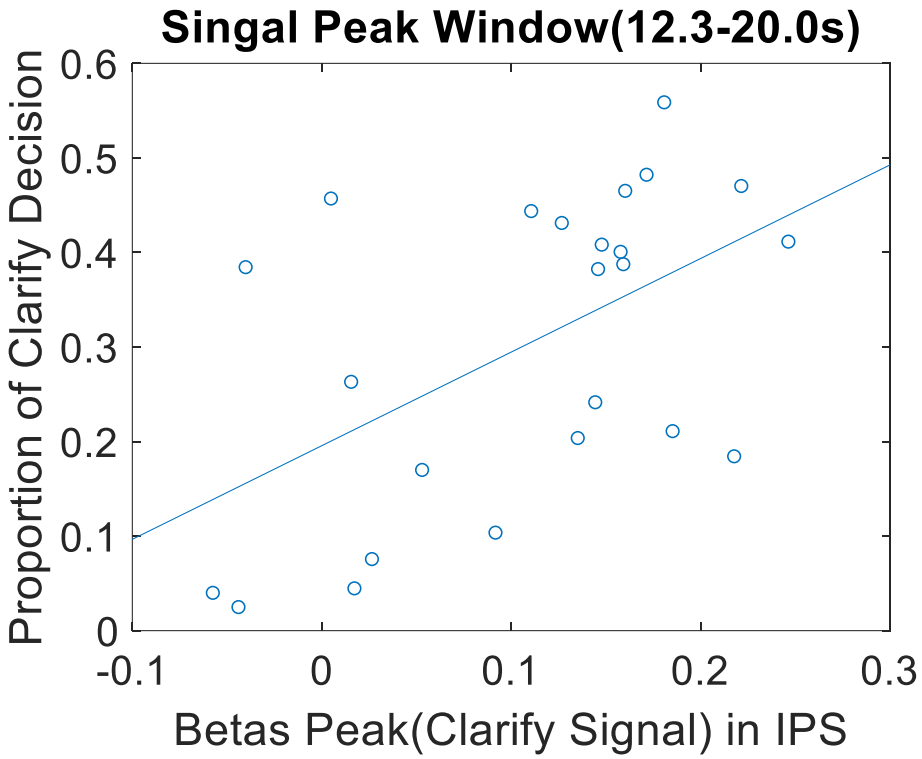

Figure 17. Individual analysis of the association between the peak of the IPS signal and the proportion of clarify decisions across subjects (N=24)

I also extracted the peak of the IPS signal from each participant to run an individual analysis and found that the size of the participants' peak signal was positively correlated with the proportion of clarify decisions made by the participants in the task (r=.535, P=0.007. Fig. 17), indicating that relatively more clarify decisions and less accept or search decisions were made by the participants when they had stronger clarify signals in their IPS.

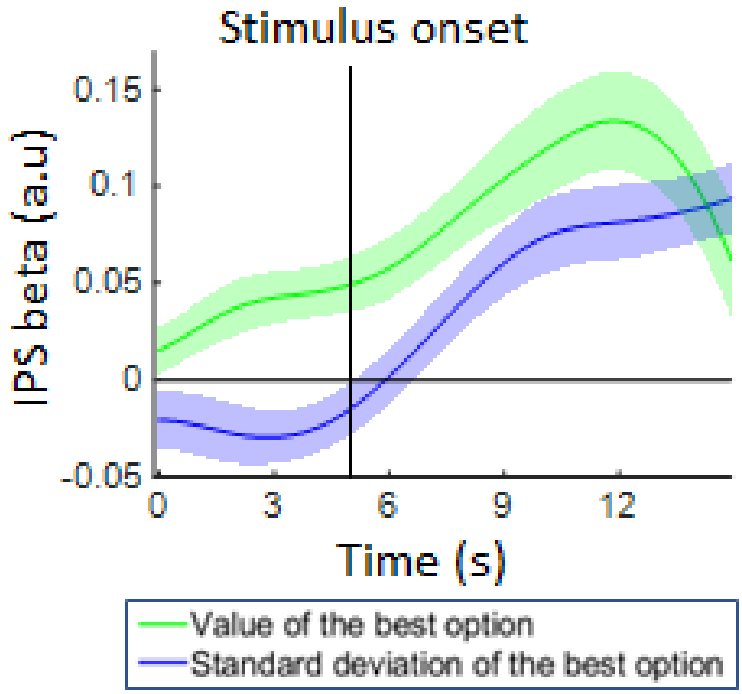

Figure 18. Critically, the IPS could signal the uncertainty of the best option. The vertical lines in the ROI time-course analysis signalled the stimuli onset at 5 s, and leave-one-out peak selection was adopted for the ROI time-course analysis.

The same as the previous vmPFC time-course analysis of the clarify value, I also further analyzed the second component of the clarify value (i.e., the uncertainty). The results showed a positive uncertainty signal in the IPS at the peak IPS BOLD β weights during 8.3 to 15.1 s ($t(23)$=4.308, P<0.001, Fig. 18). This uncertainty signal that occurred in the IPS could be suggested by the demand for information. In short, while an option involved greater uncertainty, the IPS activity became stronger which indicated that more information about the option was needed.

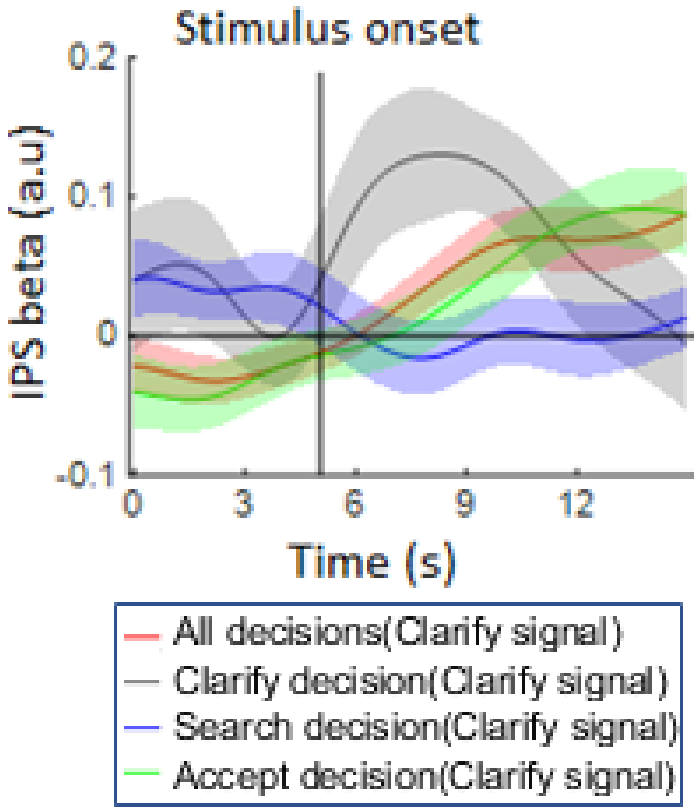

Figure 19. Subsequent ROI time-course analysis. The red clarify signal was extracted throughout the whole decision-making task, the same as the clarify signal from Fig. 15b. The grey, blue and green clarify signals were extracted while all clarify, search and accept decisions were made by the participants respectively. The vertical lines in the ROI time-course analysis signalled the stimuli onset at 5 s, and leave-one-out peak selection was adopted for the ROI time-course analysis.

To further specify the role of the IPS during clarify decisions, I conducted subsequent ROI time-course analyses for the IPS. First, I split the clarify signal (red) identified in Fig. 15b into whether the participants were making clarify decisions (grey), search decisions (blue) or accept decisions (green). The results showed that the grey clarify signal was the greatest compared with other situations which were at the peak IPS BOLD β weights during 5.6 to 11.9 s ($t(23)$=3.393, P=0.003, Fig. 19). This

also suggested that the IPS could help guide the participants to make more clarify decisions than accept or search decisions while the clarify value was greater.

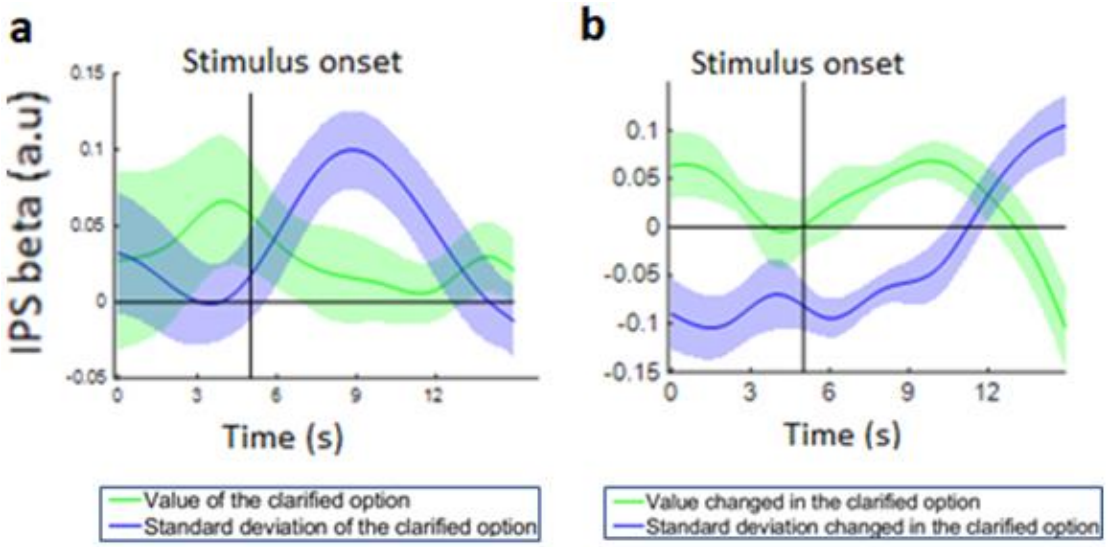

Figure 20. Subsequent ROI time-course analysis. ***a*** *IPS signals when the participants were about to make clarify decisions: a positive uncertainty signal was found in the IPS.* ***b*** *IPS signals after clarify decisions: an information gain signal was found in the IPS(blue). The vertical lines in all ROI time-course analyses signalled the stimuli onset at 5 s, and leave-one-out peak selection was adopted for all ROI time-course analyses.*

I also focused on the option that had been clarified. The results showed a positive uncertainty signal (blue) in the IPS at the peak IPS BOLD β weights during 6.2 to 12 s ($t(23)$=3.575, P=0.002, Fig. 20a), but the value signal was absent (not significant). This indicated that despite the fact that the IPS could encode the average value of the option in all situations, it preferred the uncertainty during the clarify decision-making. Apart from the previous results suggesting that the IPS is related to the demand for information, I also found that the IPS could encode information gain which was indicated by a negative signal about the change of the uncertainty of the clarified option (blue) at the peak IPS BOLD β weights during 4.1 to 10.1 s

(*t(23)*=4.474, *P*<0.001, Fig. 20b). While the clarified option became less uncertain after clarify decisions, the IPS activity became stronger. The option became more certain and indicated information gain about the possible outcome.

3.3.3 ACC and search decision

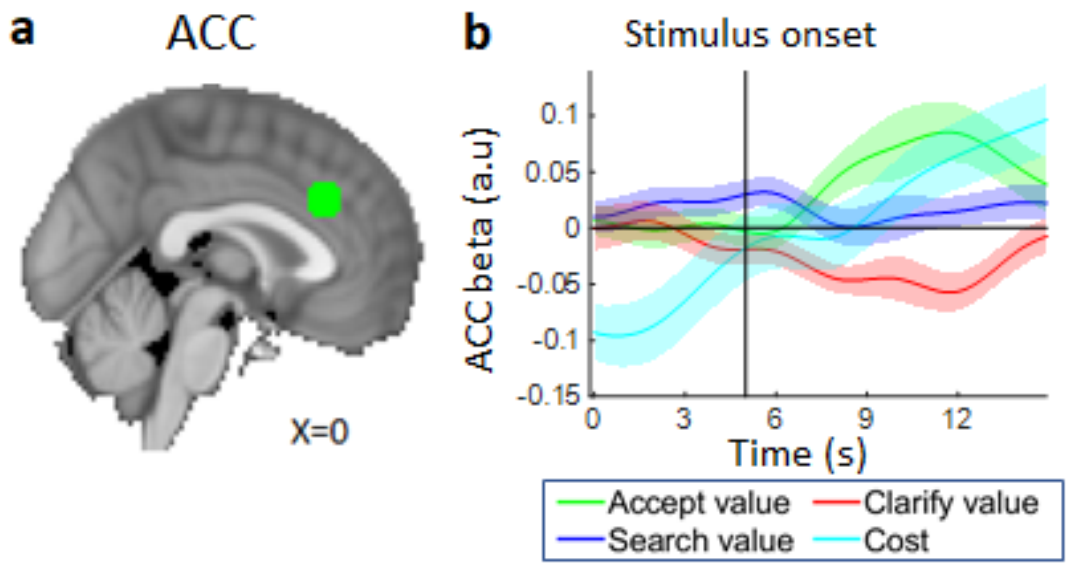

Figure 21. Analyses of the search decision. ***a*** *I defined the region (green) as the ROI for the ROI time course analyses with coordinates taken from Kolling et al. (2012).* ***b*** *A ROI time-course analysis. The three decision values and the cumulative cost estimated by the ACC activity throughout the whole decision-making task across time. A positive search signal was first found in the ACC. The vertical lines in all ROI time-course analyses signalled the stimuli onset at 5 s, and leave-one-out peak selection was adopted for all ROI time-course analyses.*

Lastly, I focused on the neural mechanisms underlying the search decision. Surprisingly, the results of the whole-brain analysis did not identify any region that was related to the search value. Since the ACC has been suggested to be related to search value by previous studies about the neural mechanisms of search behaviour

(Kolling et al., 2012, 2018), I also extracted the time course from the ACC with the coordinates shown in green (Fig. 21a) to run an ROI time-course analysis as an alternative approach to see if the clarify signal could be identified in the ACC. The accept value, clarify value, search value and cumulative cost were entered as regressors into the ROI time-course analysis to examine the association with the ACC BOLD activity across time. The results were consistent with previous findings that a positive search signal (blue) was found at the peak ACC BOLD β weights during 3.6 to 7.2 s ($t(23)$=2.254, P=0.034, Fig. 21b), which was absent in both vmPFC and IPS (Fig. 12b & 15b). However, a positive accept signal (green) at the peak ACC BOLD β weights during 7.9 to 14.8 s ($t(23)$=2.803, P=0.001, Fig. 21b) was also found. Previous findings suggest that this reflected the opportunity cost of not choosing the current option (Fouragnan et al., 2019). In this study, the accept value was the average value of the best option. It could be the opportunity cost of the search decision when the participants did not choose the best option. At the same time, a negative clarify signal (red) was found at the peak ACC BOLD β weights during 9.8 to 13.7 s ($t(23)$=-3.16, P=0.004, Fig. 21b). I therefore investigated the relationship between the ACC for search and clarify decisions, as well as search and accept decisions.

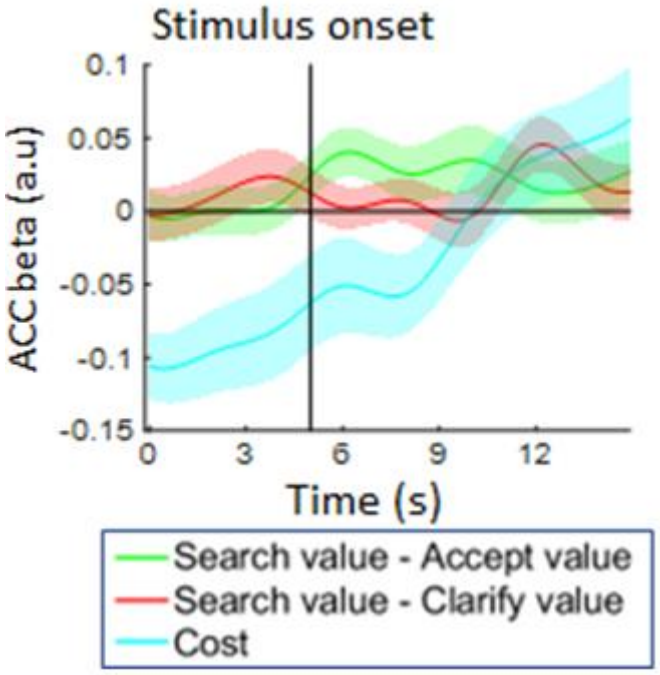

Figure 22. Subsequent ROI time-course analysis. Two value difference signals were found in the ACC, and the competition between the search and accept value first appeared, followed by the competition between the search and clarify value. The vertical lines in the ROI time-course analysis signalled the stimuli onset at 5 s, and leave-one-out peak selection was adopted for the ROI time-course analysis.

I entered two regressors into the ROI time-course analysis: search and clarify value difference (green, Fig. 22), and search and accept value difference (red, Fig. 22). Interestingly, the results showed two positive signals in the ACC (Fig. 22). First, a positive search and accept value difference signal (green) was found at the peak ACC BOLD β weights during 5.2 to 7.6 s ($t(23)$=2.252, P=0.034, Fig. 22), followed by the second peak (red), search and clarify value difference signal at the peak ACC BOLD β weights during 11.7 to 14.0 s ($t(23)$=2.367, P=0.025, Fig. 22). This suggests that when the participants made a search decision, the ACC first signalled the competition between search and accept decisions, and the competition between search and clarify decisions was signalled later.

3.4 Conclusion

In this chapter, I examined the roles of the vmPFC, IPS and ACC during accept, clarify and search decisions, respectively in multiple-choice decision-making. I found that the vmPFC encoded the value of the best option, the value difference between the best and the second-best option, and decision confidence; the IPS encoded the uncertainty of options and signalled information gain; the ACC encoded the value of searching. In short, the vmPFC, ACC and IPS all played a crucial role in accept, search and clarify decisions, respectively. However, how these three regions modulated decision formation needed to be further investigated. To address this problem, I discuss the use of a deep learning technique called Convolutional Neural Network (CNN) and Representational Similarity Analysis (RSA) in the next chapter.

Chapter 4: Convolutional Neural Network and Representational Similarity Analysis

Chapter highlights

1. This chapter aims to adopt CNN and RSA to further analyze the underlying mechanisms of information sampling in multiple-choice decision-making.
2. The trained CNN could predict 19 human decisions with an accuracy of above 87%.
3. The IPS, ACC and vmPFC showed similar computational processes to the early, intermediate and late part of the CNN during decision formation.

4.1 Introduction

In Chapter 3, I demonstrated the neural mechanisms underlying decisions of accept, clarify and search, for instance, how the defined decision values were associated with the vmPFC, IPS and ACC BOLD activities. However, it was still not clear how these three regions influenced final decision-making process. In this chapter, I will illustrate how the Convolutional Neural Network (CNN) and Representational Similarity Analysis (RSA) can be used to identify this process can be identified. CNN is a type of artificial neural network commonly used in image recognition and classification. Recently, CNN has been used in human behaviour classification (Shahverdy et al., 2020). Since the decision-making task involves integrating complex information such as option values, the environment, and costs, CNN can help visualize how this information is processed to make decisions. Additionally, RSA can compare different types of data, such as representations of the

CNN and human brain (Kriegeskorte et al., 2008), to investigate how regions of interest (ROIs) modulate decision-making. By comparing the representations in the human brain and CNN, the similarities between the two in regard to valuation and comparison processes during decision-making can be tested (Lindsay, 2020; Shahverdy et al., 2020).

4.2 Methods

4.2.1 Participants

The participants were the same as mentioned in section 2.2.1.

4.2.2 Decision-making task

The decision-making task was the same as mentioned in section 2.2.2.

4.2.3 Model architecture

The trained CNN consists of four layers. The first layer is the input layer which stores the value information of all options extracted from the decision-making task by value coding during training. The second layer is the convolutional layer with ten filters that capture low-level features and reduce the spatial size of the input without losing critical information. The outputs of this layer are called feature maps with concrete and integrated the representations. Ten convolutional filters are adopted. The third layer is the fully-connected layer. The neurons inside the fully-connected layer have full connections to all previous outputs. Three fully-connected layers are adopted. Given the lack of standardized guidelines for determining the optional number of nodes in each fully-connected layer to achieve the best model fit, it was necessary to conduct a systematic and thorough testing process. I therefore trained 11 CNNs with varying numbers of nodes in each fully-connected layer (the

power of 2, such as 32, 64, 128, 256, 512, 1024, 2048 nodes) for model comparisons. More details of the model comparisons will be discussed in Section 4.3. The last layer is the output layer, which is responsible for decision classification, using the SoftMax function to generate the choice probability of each predicted decision. The CNN predicts a total of 19 human responses, which include nine accept positions, nine clarify positions and one search decision.

4.2.4 Statistical Analysis

To find the optimal CNN architecture, 11 CNNs with varying numbers of nodes in the fully-connected layer were trained using 20-fold cross-validation to prevent overfitting. In each model, 95% of data would be used for training and 5% of data would be tested. Each data would be tested once. This resulted in 20 choice accuracies for each CNN, which were averaged and compared. The whole dataset would then be trained by using the optimal CNN architecture and that CNN was adopted for Representational Similarity Analysis (RSA) to test the similarity in the computational processes with neural data.

Prior to conducting RSA, the representational dissimilarity matrices (RDMs) were built from different types of data of each participant by pairwise comparisons of representations (the multivariate patterns) across time or the trial, and the correlations between them were then tested, such as examining the relationship between the CNN multi-nodal representations and the multi-voxel activation pattern of the ROIs.

In this study, the ROIs used in the RSA were qualified by previous univariate tests, and were extracted from the same coordinates used in previous time-course analyses. The representational dissimilarity matrices (RDMs) were built for the multi-voxel activation patterns from these ROIs (i.e., the vmPFC, ACC and IPS, left panel,

Fig. 24a). The RDMs for the CNN outputs (i.e., activations) from different layers (right panel, Fig. 24a) were also built. The RDMs of the fMRI patterns of cerebrospinal fluid (CSF), the primary visual cortex (V1) and the third visual cortex (V3) were also built as the control regions. All RSA results were indicated by the Spearman correlation coefficient and tested by Wilcoxon Signed-rank tests.

4.3 Results

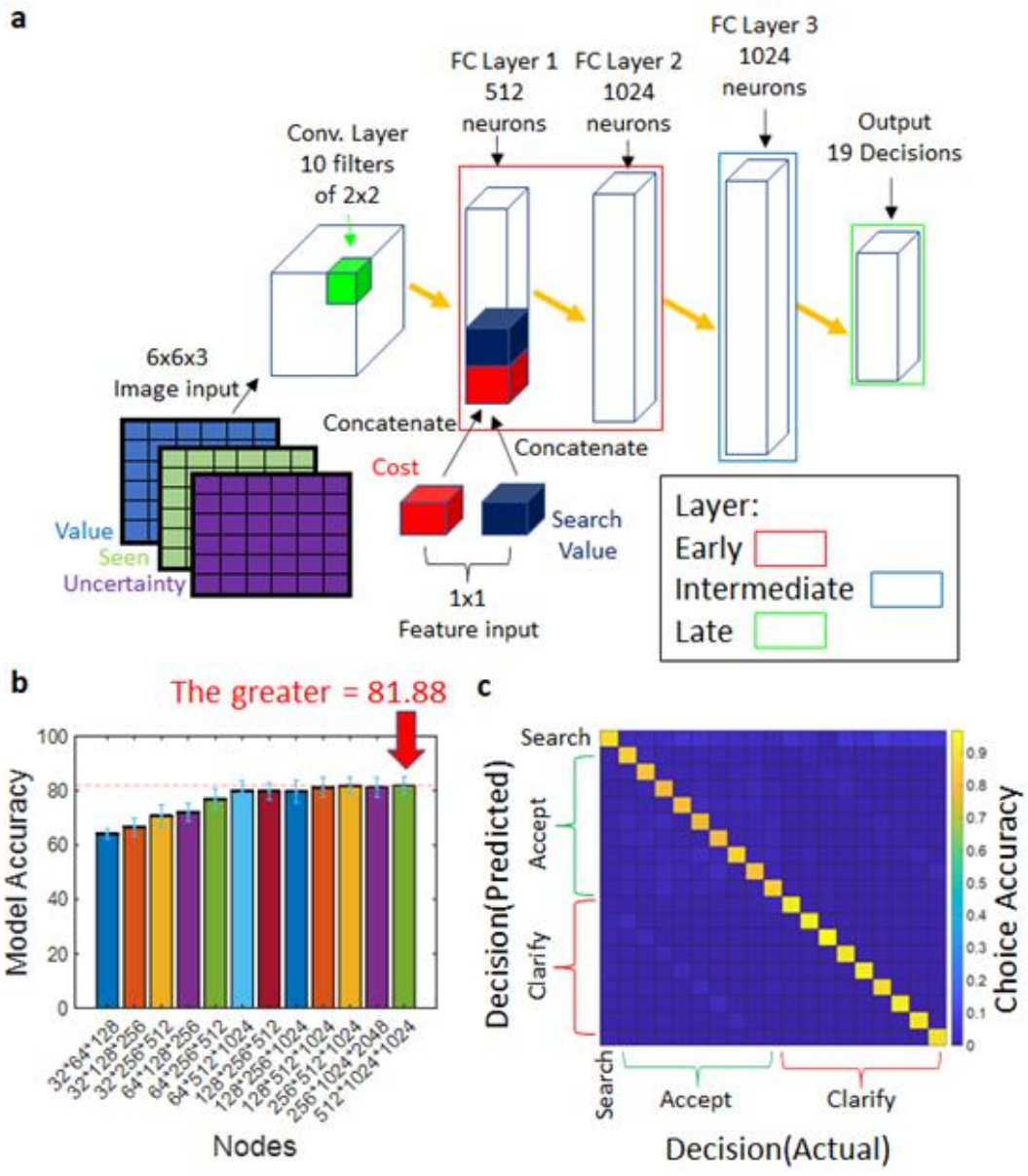

Figure 23. Convolutional Neural Network (CNN). A multi-nodal model was adopted for investigating the neural mechanisms of decision formation in the decision-making task. ***a*** *Model architecture. There are four types of layers in the CNN. The first type of layer is the input layer. All information about the option (the value of each hidden and revealed dial (i.e., value), the existence of each option, whether the option was revealed (i.e., seen), and the existence of each dial as a dial would be removed after a clarify decision (i.e., uncertainty) in the decision-making task is converged as the image input and entered into the CNN by spatial coding. The image size is 6x6 which is combined by 3x3 options and 2x2 dials for each option. The second type of layer is the convolutional layer (Conv. Layer) which captures the features of the image input. The outputs (or activations) of the Conv. Layer are then converged and entered into the third type of layer called fully-connected layer. Each fully-connected layer has full connections to all previous outputs. This process could learn the weights of each node in each fully-connected layer. Three fully-connected layers are adopted. Besides, all information about the environment (the cost incurred by each search or clarify decision (i.e., cost), and the average value of all hidden and revealed options (i.e., search value) in the decision-making task is concatenated with the outputs of the first fully-connected layer and entered into the second fully-connected layer, third fully-connected layer and to the fourth type of layer, the late layer (i.e., output or dense layer) together.* ***b*** *Model comparison, the comparisons on the average choice accuracy across models, a 20-fold cross-validation was adopted for deciding the best model with the greatest choice accuracy for the use of subsequent analyses. Standard deviation bars represent means±SD.* ***c*** *Model performance of the best model, a total of 19 choices were predicted (i.e., one search decision, nine accept positions and nine clarify positions (max. nine revealed options within a trial).*

The result showed that the optimal architecture of CNN involved 512, 1024, and 1024 nodes in the first, second and third fully-connected layer, respectively, which possessed the greatest average choice accuracy among subsets (mean=81.88, SD=3.1499. Fig. 23b), and 87.95% choice accuracy for the complete dataset (Fig. 23c). This model was then adopted to correlate with the neural data by RSA.

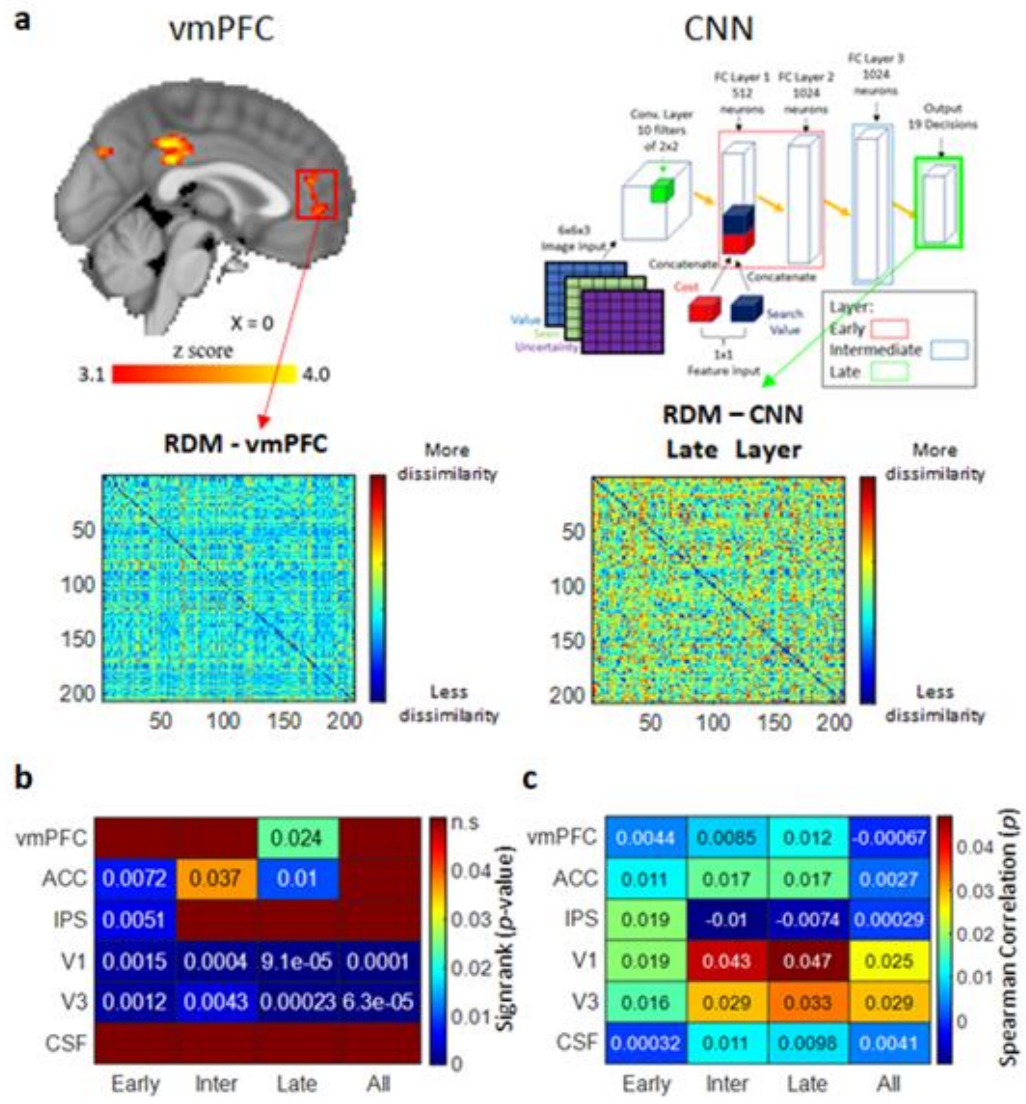

Figure 24. Representational similarity analysis (RSA): the RSA approach was adapted from Kriegeskorte et al. (2008) for investigating how human neural representations were transformed through the CNN model. ***a*** *The vmPFC, ACC, IPS activity and the activations of each layer of the CNN were used to construct their own*

representational dissimilarity matrix (RDM) by computing pairwise comparisons for each participant across trials. This process could examine the representational similarity between the human brain and deep learning model during decision formation. Examples of the RDM for vmPFC activity and the RDM for activations of the late layer are shown at the bottom. ***b*** *A p-value table for all Wilcoxon signed-rank tests for the RSA results. Each RSA was conducted for the RDM from different brains and different parts of the CNN in a subject-by-subject manner. All correlation coefficients were tested by Wilcoxon Signed-rank tests,* ***c*** *A Spearman correlation coefficient table for each RSA. The CNN was divided into three parts (i.e., the early, intermediate, and late layers) that corresponded to the number of ROIs. The layers that processed both image and feature inputs were defined as the early layer (combined the activations of fully-connected layers 1 and 2), and the layer that integrated image and feature outputs was defined as the intermediate layer. The layer that was used for decision classifications was defined as the late layer. In addition, an extra layer called "All" combined all activations from the early, intermediate and late layers.*

Interestingly, no significant correlation was found between the representations in the "All" layer and each ROI (Fig. 24b). Since different layers in the CNN are responsible for different functions, I divided the representations in the CNN of different layers and correlated with the representations of ROIs.

Critically, the results showed that the representations in the IPS (r=.019, P=0.0051) and ACC (r=.011, P=0.0072) were both positively correlated to the representations in the early layer of the CNN (Fig. 24b & 24c). The result of IPS could be suggested by the spatial coding of image input and the spatial nature of the

IPS (Leathers & Olson, 2012; Platt & Glimcher, 1999; Shadlen & Newsome, 1996) that spatial features are particularly important to be processed during the early stage of decision formation. Besides, the result of the ACC could be supported by its role in value comparison process (Boorman et al., 2013; Bush et al., 2002; Kolling et al., 2012, 2018) which was also required to integrate value information during the early stage of decision formation. Also, the representations in the ACC (r=.017, P=0.037) were also found to be positively correlated with the representations in the intermediate layer of the CNN (Fig. 24b & 24c). The results might suggest that the ACC modulates both early and late stages of decision formation, which could be suggested by the pattern of fixed connectivity of increasing value signalling began from IPS to ACC, and ACC to vmPFC (Hare et al., 2011), consisted with my results that the representations in the vmPFC (r=.012, P=0.024) and ACC (r=.017, P=0.01) were positively correlated with the representations in the late layer of the CNN (Fig. 24b & 24c).

For control analyses, the results showed that there was no significant relationship between the representations in the CSF and each part of the CNN. However, there were significant relationships between the representations in both V1, V3 and all parts of the CNN (p-value < .01 for all *Wilcoxon* Signed-rank tests, Fig. 24b), which could be suggested by the design settings of the decision-making task that the ability of perceptual processing is required. Overall, the RSA helped to visualize the representational relationship between the human brain and CNN during decision formation, suggesting their similarity in regard to valuation and comparison processing.

4.4 Conclusion

In this chapter, I illustrated how the CNN and RSA were used to understand the decision-making processes in the human brain. Through model comparisons, the optimal architecture of the CNN was defined, and the data of that CNN was tested with human brain data by RSA. The results of the RSA found that both IPS-like and ACC-like representations occurred in the early stage of the CNN during decision formation, indicating the primary processing of spatial and value information. The ACC-like representations that occurred in the intermediate stage of the CNN helped modulate both primary information processing and final decision formation. Last, both vmPFC-like and ACC-like representations occurred in the late stage of the CNN during final decision formation.

Chapter 5: General Discussion

We make numerous decisions among multiple options in our daily lives, and typically choose the option with the greatest value. Although this seems simple in words, the decision-making process is actually more complex and involves various brain processes. The vmPFC is known to be involved in valuation and value comparison processes, but sometimes we struggle to make decisions because we are unsure of the available options or wonder if there is a better option out there. For instance, we may not be certain about the outcomes, or may wonder if there is something better that has not been discovered in the environment (Badre et al., 2012). I suggest two types of information sampling processes to address this problem, which are sampling information from options and environments. The former process aims to clarify the options to reduce the uncertainties, in which no new options would be discovered, while the latter process aims to search for alternatives from the environment, in which new options would be discovered. Previous evidence suggests that the IPS and ACC are crucial with these processes, respectively.

Although previous literature provides neural evidence about information sampling, the central problem of this thesis is that there are three types of decisions that we need to consider at the same time, which are selecting better options and two types of information sampling, while the dynamics of these decisions have not been investigated.

As mentioned in **Chapter 1**, the motives of information sampling could be sophisticated and stochastic (Blanchard & Gershman, 2017). The neural mechanisms are still being investigated. Recent evidence suggests that the IPS is related to the

demand for information and information gain (Foley et al., 2017; Gottlieb, 2018; Gottlieb et al., 2014; Gottlieb & Oudeyer, 2018; Horan et al., 2019), while the ACC is related to the value of sampling and sampling cost (Kolling et al., 2012, 2018). Interestingly, both the IPS and ACC are seldom discussed together in researches on information sampling, as most of them might largely focused while animal subjects sampled information from options or environments independently. For instance, the IPS is discussed more when the experimental task is about sampling information from options to reduce the uncertainties, while the ACC is discussed more when it comes to sampling information from the environment to discover more alternatives. However, real-life examples suggest that we usually decide between sampling options and environments at the same time. Moreover, most of the relevant studies focused more on binary-choice decision-making, while real-life examples suggest that usually there are multiple options to be compared. It is important to study the neural mechanisms of information sampling in multiple-choice decision-making as they remain unclear. In this thesis, I review and define three candidate regions (i.e., the vmPFC, IPS and ACC) and tested their roles during information sampling in multiple-choice decision-making.

To address the problem of investigating the neural mechanisms of information sampling in multiple-choice decision-making, I designed a multiple-choice decision-making task which was adopted in **Chapters 2-4**. During the designed decision-making task, people were required to decide between three possible decisions (i.e., *accept*, to obtain the value of a selected option; *clarify*, to sample information from an option to reduce uncertainty; *search*, to sample information from the environment, so a new option would be discovered). In **Chapter 3**, I reported an fMRI experiment and showed the roles of the vmPFC, IPS and ACC during decisions of accept, clarify

and search, respectively. I showed that the vmPFC signals the average value of the best option. Critically, it also signals the value difference between the average value of the best option and the second-best option, which helps signal the better option and guides the accept decision during the decision-making task. The results were consistent with previous studies that the vmPFC encodes value differences between chosen and unchosen options (the best option is usually the chosen option while the second-best option is the unchosen option) (Boorman et al., 2013). However, the same analysis of the IPS showed the opposite result. The IPS could only signal the average value of the best option but not the second-best option. The results might suggest that the IPS is only involved in the valuation process but not the value comparison process. This could be supported by early literature in that the IPS was found to be able to encode the subjective value in perceptual decision-making tasks (Leathers & Olson, 2012; Platt & Glimcher, 1999).

While the IPS was found to be crucial during the sampling of information from options, I showed that the IPS positively signals the uncertainty of both the best option and the options that are selected to be clarified, while the same analyses in the vmPFC showed opposite results. The results might suggest that the greater uncertainty of options decreases our decision confidence to accept them as the outcomes of their options are more unpredictable (Hebscher & Gilboa, 2016; Shapiro & Grafton, 2020). Critically, I also showed that the positive clarify signal in the IPS is the strongest when making a clarify decision. Since the clarify signal is composed of the average value and the uncertainty of an option, I further showed that the IPS activities are mainly associated with the uncertainty but not the average value of the clarified options, indicating that the IPS guides clarify decisions based on the uncertainty more. As a greater uncertainty indicates that more information is needed, the results were

consistent with previous studies that the IPS signals the demand for information. I also showed that the IPS can signal information gain (Foley et al., 2017; Gottlieb, 2018; Gottlieb et al., 2014; Gottlieb & Oudeyer, 2018; Horan et al., 2019). While the uncertainty of options becomes smaller after clarify decisions are made, the IPS activities become stronger.

I then also showed that the ACC plays a critical role in the sampling of information from the environment. The ACC is the only candidate region that can positively encode the search value (Hunt et al., 2012; Juni, Gureckis & Maloney, 2016). Critically, I also showed that the ACC encodes two value comparison signals, in which the comparison between search and accept decisions is first processed, followed by the comparison between search and clarify decisions. The results might suggest that the ACC guides search decisions while the values of both accept and clarify decisions need to be relatively unappealing compared with the search value. Interestingly, the ACC prioritizes the comparison of accept decisions over clarify decisions. This could be suggested by the role of the ACC that it also encodes an inverse value difference between chosen and unchosen options (Kolling et al., 2012). The value of the best option and the search value could be defined as the values of chosen and unchosen options, respectively. If the search value is smaller than the value of the best option, a search decision is not preferred and would be signalled in the early stage of decision formation.

To investigate how the vmPFC, IPS and ACC formulated the final decision between three possible decisions in the designed decision-making task, I also employed the CNN and conducted a series of RSA to visualize the functional pathway of these three regions in **Chapter 4**. The approach of employing both the CNN and

RSA has been recently used as computational theories of the human brain (Cross et al., 2021; Flesch et al., 2022). I extracted the multi-nodal representations from the CNN with the highest accuracy (87.95% for predicting 19 responses) for comparison with the multi-voxel activation patterns of the vmPFC, IPS and ACC. Critically, while previous studies largely focused on the comparison between the entire CNN with only a single brain region (Cross et al., 2021; Flesch et al., 2022), my study showed that the vmPFC, ACC and IPS only have similar representations in early, intermediate and late parts of the CNN but not the entire CNN, which are responsible for feature extraction, integration and decision making, respectively. The results might suggest the feasibility of conducting a series of RSA on the subparts of other deep learning models including more brain regions to investigate the neuro-computational mechanisms of decision-making.

5.1 General Conclusions

This thesis sheds light on the neural mechanisms underlying information sampling in multiple-choice decision-making, which the vmPFC, IPS and ACC are identified as key regions with distinct roles. The vmPFC is critical in selecting the best options, by encoding the difference between the values of the options. Meanwhile, the IPS and ACC are both critical in the process of information sampling. The IPS guides the sampling of information from existing options by encoding their level of uncertainty, while the ACC guides the sampling of information from the environment by encoding the value of searching. Besides, utilizing both CNN and RSA helps to visualize the functional pathway of the vmPFC, IPS and ACC during information sampling in multiple-choice decision-making. The IPS, ACC and vmPFC are more related to the early, intermediate and late stages of decision formation

respectively. This thesis reveals the unified framework to illustrate the dynamics between option selection process and information sampling processes.

References

Albantakis, L., & Deco, G. (2009). The encoding of alternatives in multiple-choice decision-making. *BMC Neuroscience*, *10*(S1), 2008. https://doi.org/10.1186/1471-2202-10-s1-p166

Badre, D., Doll, B. B., Long, N. M., & Frank, M. J. (2012). Rostrolateral prefrontal cortex and individual differences in uncertainty-driven exploration. *Neuron*, *73*(3), 595–607. https://doi.org/10.1016/j.neuron.2011.12.025

Bartra, O., McGuire, J. T., & Kable, J. W. (2013). The valuation system: A coordinate-based meta-analysis of BOLD fMRI experiments examining neural correlates of subjective value. *NeuroImage*, *76*, 412–427. https://doi.org/10.1016/j.neuroimage.2013.02.063

Bayer, H. M., & Glimcher, P. W. (2005). Midbrain dopamine neurons encode a quantitative reward prediction error signal. *Neuron*, *47*(1), 129–141. https://doi.org/10.1016/j.neuron.2005.05.020

Beckmann, C. F., Jenkinson, M., & Smith, S. M. (2003). General multilevel linear modeling for group analysis in FMRI. *NeuroImage*, *20*(2), 1052–1063. https://doi.org/10.1016/S1053-8119(03)00435-X

Beckmann, M., Johansen-Berg, H., & Rushworth, M. F. S. (2009). Connectivity-based parcellation of human cingulate cortex and its relation to functional specialization. *Journal of Neuroscience*, *29*(4), 1175–1190. https://doi.org/10.1523/JNEUROSCI.3328-08.2009

Behrens, T. E. J., Woolrich, M. W., Walton, M. E., & Rushworth, M. F. S. (2007).

Learning the value of information in an uncertain world. *Nature Neuroscience*, *10*(9), 1214–1221. https://doi.org/10.1038/nn1954

Blair, K., Marsh, A. A., Morton, J., Vythilingam, M., Jones, M., Mondillo, K., Pine, D. C., Drevets, W. C., & Blair, J. R. (2006). Choosing the lesser of two evils, the better of two goods: Specifying the roles of ventromedial prefrontal cortex and dorsal anterior cingulate in object choice. *Journal of Neuroscience*, *26*(44), 11379–11386. https://doi.org/10.1523/JNEUROSCI.1640-06.2006

Blanchard, T. C., & Gershman, S. J. (2017). Pure Correlates of Exploration and Exploitation in the Human Brain. *BioRxiv*. https://doi.org/10.1101/103135

Bonaiuto, J. J., De Berker, A., & Bestmann, S. (2016). Response repetition biases in human perceptual decisions are explained by activity decay in competitive attractor models. *ELife*, *5*(DECEMBER2016), 1–28. https://doi.org/10.7554/eLife.20047

Bonnici, H. M., Chadwick, M. J., Lutti, A., Hassabis, D., Weiskopf, N., & Maguire, E. A. (2012). Detecting representations of recent and remote autobiographical memories in vmPFC and hippocampus. *Journal of Neuroscience*, *32*(47), 16982–16991. https://doi.org/10.1523/JNEUROSCI.2475-12.2012

Bontempi, B., Laurent-Demir, C., Destrade, C., & Jaffard, R. (1999). Time-dependent reorganization of brain circuitry underlying long-term memory storage. *Nature*, *400*(6745), 671–675. https://doi.org/10.1038/23270

Boorman, E. D., Rushworth, M. F., & Behrens, T. E. (2013). Ventromedial prefrontal and anterior cingulate cortex adopt choice and default reference frames during sequential multi-alternative choice. *Journal of Neuroscience*, *33*(6), 2242–2253.

https://doi.org/10.1523/JNEUROSCI.3022-12.2013

Bush, G., Vogt, B. A., Holmes, J., Dale, A. M., Greve, D., Jenike, M. A., & Rosen, B. R. (2002). Dorsal anterior cingulate cortex: A role in reward-based decision making. *Proceedings of the National Academy of Sciences of the United States of America*, *99*(1), 523–528. https://doi.org/10.1073/pnas.012470999

Cabeza, R., Ciaramelli, E., Olson, I. R., & Moscovitch, M. (2008). The parietal cortex and episodic memory: An attentional account. *Nature Reviews Neuroscience*, *9*(8), 613–625. https://doi.org/10.1038/nrn2459

Chau, B. K. H., Kolling, N., Hunt, L. T., Walton, M. E., & Rushworth, M. F. S. (2014). A neural mechanism underlying failure of optimal choice with multiple alternatives. *Nature Neuroscience*, *17*(3), 463–470. https://doi.org/10.1038/nn.3649

Coutlee, C. G., Kiyonaga, A., Korb, F. M., Huettel, S. A., & Egner, T. (2016). Reduced risk-taking following disruption of the intraparietal sulcus. *Frontiers in Neuroscience*, *10*(DEC), 1–9. https://doi.org/10.3389/fnins.2016.00588

Cross, L., Cockburn, J., Yue, Y., & O'Doherty, J. P. (2021). Using deep reinforcement learning to reveal how the brain encodes abstract state-space representations in high-dimensional environments. *Neuron*, *109*(4), 724-738.e7. https://doi.org/10.1016/j.neuron.2020.11.021

Donoso, M., Collins, A. G. E., & Koechlin, E. (2014). Foundations of human reasoning in the prefrontal cortex. *Science*, *344*(6191), 1481–1486. https://doi.org/10.1126/science.1252254

Drugowitsch, J., Moreno-Bote, R. N., Churchland, A. K., Shadlen, M. N., & Pouget,

A. (2012). The cost of accumulating evidence in perceptual decision making. *Journal of Neuroscience*, *32*(11), 3612–3628. https://doi.org/10.1523/JNEUROSCI.4010-11.2012

Edwards, W. (1965). Optimal strategies for seeking information: Models for statistics, choice reaction times, and human information processing. *Journal of Mathematical Psychology*, *2*(2), 312–329. https://doi.org/10.1016/0022-2496(65)90007-6

Fellows, L. K. (2011). Orbitofrontal contributions to value-based decision making: Evidence from humans with frontal lobe damage. *Annals of the New York Academy of Sciences*, *1239*(1), 51–58. https://doi.org/10.1111/j.1749-6632.2011.06229.x

Flesch, T., Juechems, K., Dumbalska, T., Saxe, A., & Summerfield, C. (2022). Orthogonal representations for robust context-dependent task performance in brains and neural networks. *Neuron*, 1–13. https://doi.org/10.1016/j.neuron.2022.01.005

Foley, N. C., Kelly, S. P., Mhatre, H., Lopes, M., & Gottlieb, J. (2017). Parietal neurons encode expected gains in instrumental information. *Proceedings of the National Academy of Sciences of the United States of America*, *114*(16), E3315–E3323. https://doi.org/10.1073/pnas.1613844114

Fouragnan, E. F., Chau, B. K. H., Folloni, D., Kolling, N., Verhagen, L., Klein-Flügge, M., Tankelevitch, L., Papageorgiou, G. K., Aubry, J. F., Sallet, J., & Rushworth, M. F. S. (2019). The macaque anterior cingulate cortex translates counterfactual choice value into actual behavioral change. *Nature Neuroscience*, *22*(5), 797–808. https://doi.org/10.1038/s41593-019-0375-6

Frankland, P. W., & Bontempi, B. (2005). The organization of recent and remote memories. *Nature Reviews Neuroscience*, *6*(2), 119–130. https://doi.org/10.1038/nrn1607

Freidin, E., & Kacelnik, A. (2011). Rational choice, context dependence, and the value of information in European starlings (Sturnus vulgaris). *Science*, *334*(6058), 1000–1002. https://doi.org/10.1126/science.1209626

Furman, M., & Wang, X. J. (2008). Similarity Effect and Optimal Control of Multiple-Choice Decision Making. *Neuron*, *60*(6), 1153–1168. https://doi.org/10.1016/j.neuron.2008.12.003

Gläscher, J., Hampton, A. N., & O'Doherty, J. P. (2009). Determining a role for ventromedial prefrontal cortex in encoding action-based value signals during reward-related decision making. *Cerebral Cortex*, *19*(2), 483–495. https://doi.org/10.1093/cercor/bhn098

Gold, J. I., & Shadlen, M. N. (2007). The neural basis of decision making. *Annual Review of Neuroscience, 30,* 535–574. https://doi.org/10.1146/annurev.neuro.29.051605.113038

Goldberg, M. E., Bisley, J., Powell, K. D., Gottlieb, J., & Kusunoki, M. (2002). The role of the lateral intraparietal area of the monkey in the generation of saccades and visuospatial attention. *Annals of the New York Academy of Sciences, 956,* 205–215. https://doi.org/10.1111/j.1749-6632.2002.tb02820.x

Gottlieb, J. (2018). Understanding active sampling strategies: Empirical approaches and implications for attention and decision research. *Cortex, 102,* 150–160. https://doi.org/10.1016/j.cortex.2017.08.019

Gottlieb, J., Hayhoe, M., Hikosaka, O., & Rangel, A. (2014). Attention, reward, and information seeking. *Journal of Neuroscience*, *34*(46), 15497–15504. https://doi.org/10.1523/JNEUROSCI.3270-14.2014

Gottlieb, J., & Oudeyer, P. Y. (2018). Towards a neuroscience of active sampling and curiosity. *Nature Reviews Neuroscience*, *19*(12), 758–770. https://doi.org/10.1038/s41583-018-0078-0

Grefkes, C., & Fink, G. R. (2005). The functional organization of the intraparietal sulcus in humans and monkeys. *Journal of Anatomy*, *207*(1), 3–17. https://doi.org/10.1111/j.1469-7580.2005.00426.x

Guo, L., Trueblood, J. S., & Diederich, A. (2017). Thinking Fast Increases Framing Effects in Risky Decision Making. *Psychological Science*, *28*(4), 530–543. https://doi.org/10.1177/0956797616689092

Hämmerer, D., Bonaiuto, J., Klein-Flügge, M., Bikson, M., & Bestmann, S. (2016). Selective alteration of human value decisions with medial frontal tDCS is predicted by changes in attractor dynamics. *Scientific Reports*, *6*(May), 1–13. https://doi.org/10.1038/srep25160

Hampton, A. N., Bossaerts, P., & O'Doherty, J. P. (2006). The role of the ventromedial prefrontal cortex in abstract state-based inference during decision making in humans. *Journal of Neuroscience*, *26*(32), 8360–8367. https://doi.org/10.1523/JNEUROSCI.1010-06.2006

Hanks, T. D., Ditterich, J., & Shadlen, M. N. (2006). Microstimulation of macaque area LIP affects decision-making in a motion discrimination task. *Nature Neuroscience*, *9*(5), 682–689. https://doi.org/10.1038/nn1683

Hänsel, A., & von Känel, R. (2008). The ventro-medial prefrontal cortex: A major link between the autonomic nervous system, regulation of emotion, and stress reactivity? *BioPsychoSocial Medicine*, *2*, 1–5. https://doi.org/10.1186/1751-0759-2-21

Hare, T. A., Schultz, W., Camerer, C. F., O'Doherty, J. P., & Rangel, A. (2011). Transformation of stimulus value signals into motor commands during simple choice. *Proceedings of the National Academy of Sciences of the United States of America*, *108*(44), 18120–18125. https://doi.org/10.1073/pnas.1109322108

Hebscher, M., & Gilboa, A. (2016). A boost of confidence: The role of the ventromedial prefrontal cortex in memory, decision-making, and schemas. *Neuropsychologia*, *90*(1989), 46–58. https://doi.org/10.1016/j.neuropsychologia.2016.05.003

Horan, M., Daddaoua, N., & Gottlieb, J. (2019). Parietal neurons encode information sampling based on decision uncertainty. *Nature Neuroscience*, *22*(8), 1327–1335. https://doi.org/10.1038/s41593-019-0440-1

Huettel, S. A., Stowe, C. J., Gordon, E. M., Warner, B. T., & Platt, M. L. (2006). Neural signatures of economic preferences for risk and ambiguity. *Neuron*, *49*(5), 765–775. https://doi.org/10.1016/j.neuron.2006.01.024

Hunt, L. T., Kolling, N., Soltani, A., Woolrich, M. W., Rushworth, M. F. S., & Behrens, T. E. J. (2012). Mechanisms underlying cortical activity during value-guided choice. *Nature Neuroscience*, *15*(3), 470–476. https://doi.org/10.1038/nn.3017

Hunt, L. T., Rutledge, R. B., Malalasekera, W. M. N., Kennerley, S. W., & Dolan, R.

J. (2016). Approach-Induced Biases in Human Information Sampling. *PLoS Biology*, *14*(11), 1–23. https://doi.org/10.1371/journal.pbio.2000638

Hunt, L. T., Woolrich, M. W., Rushworth, M. F. S., & Behrens, T. E. J. (2013). Trial-Type Dependent Frames of Reference for Value Comparison. *PLoS Computational Biology*, *9*(9). https://doi.org/10.1371/journal.pcbi.1003225

Jenkinson, M. (2003). Fast, automated, N-dimensional phase-unwrapping algorithm. *Magnetic Resonance in Medicine*, *49*(1), 193–197. https://doi.org/10.1002/mrm.10354

Jenkinson, M., Bannister, P., Brady, M., & Smith, S. (2002). Improved Optimization for the Robust and Accurate Linear Registration and Motion Correction of Brain Images. *NeuroImage*, *17*(2), 825–841. https://doi.org/10.1006/nimg.2002.1132

Jenkinson, M., & Smith, S. (2001). A global optimisation method for robust affine registration of brain images. *Medical Image Analysis*, *5*(2), 143–156. https://doi.org/10.1016/S1361-8415(01)00036-6

Jocham, G., Hunt, L. T., Near, J., & Behrens, T. E. J. (2012). A mechanism for value-guided choice based on the excitation-inhibition balance in prefrontal cortex. *Nature Neuroscience*, *15*(7), 960–961. https://doi.org/10.1038/nn.3140

Juni, M. Z., Gureckis, T. M., & Maloney, L. T. (2016). Information sampling behavior with explicit sampling costs. *Decision*, *3*(3), 147–168. https://doi.org/10.1037/dec0000045

Kable, J. W., & Glimcher, P. W. (2009). The Neurobiology of Decision: Consensus and Controversy. *Neuron*, *63*(6), 733–745. https://doi.org/10.1016/j.neuron.2009.09.003

Kennerley, S. W., Walton, M. E., Behrens, T. E. J., Buckley, M. J., & Rushworth, M. F. S. (2006). Optimal decision making and the anterior cingulate cortex. *Nature Neuroscience*, *9*(7), 940–947. https://doi.org/10.1038/nn1724

Kiani, R., & Shadlen, M. N. (2009). Representation of confidence associated with a decision by neurons in the parietal cortex. *Science*, *324*(5928), 759–764. https://doi.org/10.1126/science.1169405

Knox, W. B., Otto, A. R., Stone, P., & Love, B. C. (2011). The nature of belief-directed exploratory choice in human decision-making. *Frontiers in Psychology*, *2*(JAN), 1–12. https://doi.org/10.3389/fpsyg.2011.00398

Kolling, N., Behrens, T. E. J., Mars, R. B., & Rushworth, M. F. S. (2012). Neural mechanisms of foraging. *Science*, *335*(6077), 95–98. https://doi.org/10.1126/science.1216930

Kolling, N., Scholl, J., Chekroud, A., Trier, H. A., & Rushworth, M. F. S. (2018). Prospection, Perseverance, and Insight in Sequential Behavior. *Neuron*, *99*(5), 1069-1082.e7. https://doi.org/10.1016/j.neuron.2018.08.018

Koutsarnakis, C., Liakos, F., Kalyvas, A. V., Liouta, E., Emelifeonwu, J., Kalamatianos, T., Sakas, D. E., Johnson, E., & Stranjalis, G. (2017). Approaching the atrium through the intraparietal sulcus: Mapping the sulcal morphology and correlating the surgical corridor to underlying fiber tracts. *Operative Neurosurgery*, *13*(4), 503–516. https://doi.org/10.1093/ons/opw037

Kriegeskorte, N., Mur, M., & Bandettini, P. (2008). Representational similarity analysis - connecting the branches of systems neuroscience. *Frontiers in Systems Neuroscience*, *2*(NOV), 1–28. https://doi.org/10.3389/neuro.06.004.2008

Kurniawan, I. T., Guitart-Masip, M., Dayan, P., & Dolan, R. J. (2013). Effort and valuation in the brain: The effects of anticipation and execution. *Journal of Neuroscience*, *33*(14), 6160–6169. https://doi.org/10.1523/JNEUROSCI.4777-12.2013

Leathers, M. L., & Olson, C. R. (2012). In Monkeys Making Value-Based Decisions, LIP Neurons Encode Cue Salience and Not Action Value. *Science*, *338*(October), 132–135. http://www.sciencemag.org/content/338/6103/132%5Cnhttp://www.sciencemag.org/content/338/6103/132.full%5Cnhttp://www.sciencemag.org/content/338/6103/132.full.pdf%5Cnhttp://www.pubmedcentral.nih.gov/articlerender.fcgi?artid=3705639&tool=pmcentrez&rendertype

Lebreton, M., Jorge, S., Michel, V., Thirion, B., & Pessiglione, M. (2009). An Automatic Valuation System in the Human Brain: Evidence from Functional Neuroimaging. *Neuron*, *64*(3), 431–439. https://doi.org/10.1016/j.neuron.2009.09.040

Levy, D. J., & Glimcher, P. W. (2012). The root of all value: A neural common currency for choice. *Current Opinion in Neurobiology*, *22*(6), 1027–1038. https://doi.org/10.1016/j.conb.2012.06.001

Lindsay, G. W. (2020). Convolutional Neural Networks as a Model of the Visual System: Past, Present, and Future. *ArXiv*. https://doi.org/10.1162/jocn_a_01544

Lopez-Persem, A., Verhagen, L., Amiez, C., Petrides, M., & Sallet, J. (2019). The human ventromedial prefrontal cortex: Sulcal morphology and its influence on functional organization. *Journal of Neuroscience*, *39*(19), 3627–3639. https://doi.org/10.1523/JNEUROSCI.2060-18.2019

Margulies, D. S., Kelly, A. M. C., Uddin, L. Q., Biswal, B. B., Castellanos, F. X., & Milham, M. P. (2007). Mapping the functional connectivity of anterior cingulate cortex. *NeuroImage*, *37*(2), 579–588. https://doi.org/10.1016/j.neuroimage.2007.05.019

Marois, R., & Todd, J. J. (2004). Capacity limit of visual short-term memory in human posterior parietal cortex. *Nature*, *428*, 751—754.

Mars, R. B., Jbabdi, S., Sallet, J., O'Reilly, J. X., Croxson, P. L., Olivier, E., Noonan, M. A. P., Bergmann, C., Mitchell, A. S., Baxter, M. G., Behrens, T. E. J., Johansen-Berg, H., Tomassini, V., Miller, K. L., & Rushworth, M. F. S. (2011). Diffusion-weighted imaging tractography-based parcellation of the human parietal cortex and comparison with human and macaque resting-state functional connectivity. *Journal of Neuroscience*, *31*(11), 4087–4100. https://doi.org/10.1523/JNEUROSCI.5102-10.2011

Milosavljevic, M., Malmaud, J., Huth, A., Koch, C., & Rangel, A. (2010). The Drift Diffusion Model can account for the accuracy and reaction time of value-based choices under high and low time pressure. *Judgment and Decision Making*, *5*(6), 437–449. https://doi.org/10.2139/ssrn.1901533

Molko, N., Cachia, A., Rivière, D., Mangin, J. F., Bruandet, M., Le Bihan, D., Cohen, L., & Dehaene, S. (2003). Functional and structural alterations of the intraparietal sulcus in a developmental dyscalculia of genetic origin. *Neuron*, *40*(4), 847–858. https://doi.org/10.1016/S0896-6273(03)00670-6

Montague, P. R., Dayan, P., & Sejnowski, T. J. (1996). A framework for mesencephalic dopamine systems based on predictive Hebbian learning. *Journal of Neuroscience*, *16*(5), 1936–1947. https://doi.org/10.1523/jneurosci.16-05-

01936.1996

Mooney, H. A., & Cleland, E. E. (2001). The evolutionary impact of invasive species. *Proceedings of the National Academy of Sciences of the United States of America*, *98*(10), 5446–5451. https://doi.org/10.1073/pnas.091093398

Paholpak, P., & Mendez, M. F. (2016). Apathy: Frontal and Basal Ganglia Circuits. In *Genomics, Circuits, and Pathways in Clinical Neuropsychiatry*. Elsevier Inc. https://doi.org/10.1016/B978-0-12-800105-9.00021-4

Palomero-Gallagher, N., Vogt, B. A., Schleicher, A., Mayberg, H. S., & Zilles, K. (2009). Receptor architecture of human cingulate cortex: Evaluation of the four-region neurobiological model. *Human Brain Mapping*, *30*(8), 2336–2355. https://doi.org/10.1002/hbm.20667

Pearson, J. M., Watson, K. K., & Platt, M. L. (2014). Decision making: The neuroethological turn. *Neuron*, *82*(5), 950–965. https://doi.org/10.1016/j.neuron.2014.04.037

Pessoa, L. (2008). On the relationship between emotion and cognition. *Nature Reviews Neuroscience*, *9*(Box 2), 148–158.

Platt, M. L., & Glimcher, P. W. (1999). Neural correlates of decision variables in parietal cortex. *Nature*, *400*(6741), 233–238. https://doi.org/10.1038/22268

Quilodran, R., Rothé, M., & Procyk, E. (2008). Behavioral Shifts and Action Valuation in the Anterior Cingulate Cortex. *Neuron*, *57*(2), 314–325. https://doi.org/10.1016/j.neuron.2007.11.031

Rangel, A., & Hare, T. (2010). Neural computations associated with goal-directed choice. *Current Opinion in Neurobiology*, *20*(2), 262–270.

https://doi.org/10.1016/j.conb.2010.03.001

Ratcliff, R. (1978). A theory of memory retrieval. *Psychological Review*, *85*(2), 59–108. https://doi.org/10.1037/0033-295X.85.2.59

Ratcliff, R., Hasegawa, Y. T., Hasegawa, R. P., Smith, P. L., & Segraves, M. A. (2007). Dual diffusion model for single-cell recording data from the superior colliculus in a brightness-discrimination task. *Journal of Neurophysiology*, *97*(2), 1756–1774. https://doi.org/10.1152/jn.00393.2006

Reitich-Stolero, T., Aberg, K. C., & Paz, R. (2019). Re-exploring Mechanisms of Exploration. *Neuron*, *103*(3), 360–363. https://doi.org/10.1016/j.neuron.2019.07.021

Rolls, E. T., Huang, C. C., Lin, C. P., Feng, J., & Joliot, M. (2020). Automated anatomical labelling atlas 3. *NeuroImage*, *206*(May), 116189. https://doi.org/10.1016/j.neuroimage.2019.116189

Rudebeck, P. H., & Murray, E. A. (2011). Dissociable effects of subtotal lesions within the macaque orbital prefrontal cortex on reward-guided behavior. *Journal of Neuroscience*, *31*(29), 10569–10578. https://doi.org/10.1523/JNEUROSCI.0091-11.2011

Schwarz, G. (1978). Estimating the Dimension of a Model. In *The Annals of Statistics* (Vol. 6, Issue 2). https://doi.org/10.1214/aos/1176344136

Shadlen, M. N., & Newsome, W. T. (1996). Motion perception: Seeing and deciding. *Proceedings of the National Academy of Sciences of the United States of America*, *93*(2), 628–633. https://doi.org/10.1073/pnas.93.2.628

Shadlen, M. N., & Newsome, W. T. (2001). Neural basis of a perceptual decision in

the parietal cortex (area LIP) of the rhesus monkey. *Journal of Neurophysiology*, *86*(4), 1916–1936. https://doi.org/10.1152/jn.2001.86.4.1916

Shahverdy, M., Fathy, M., Berangi, R., & Sabokrou, M. (2020). Driver behavior detection and classification using deep convolutional neural networks. *Expert Systems with Applications*, *149*, 113240. https://doi.org/10.1016/j.eswa.2020.113240

Shapiro, A. D., & Grafton, S. T. (2020). Subjective value then confidence in human ventromedial prefrontal cortex. *PLoS ONE*, *15*(2), 1–28. https://doi.org/10.1371/journal.pone.0225617

Smith, S. M. (2002). Fast robust automated brain extraction. *Human Brain Mapping*, *17*(3), 143–155. https://doi.org/10.1002/hbm.10062

Smith, S. M., Jenkinson, M., Woolrich, M. W., Beckmann, C. F., Behrens, T. E. J., Johansen-Berg, H., Bannister, P. R., De Luca, M., Drobnjak, I., Flitney, D. E., Niazy, R. K., Saunders, J., Vickers, J., Zhang, Y., De Stefano, N., Brady, J. M., & Matthews, P. M. (2004). Advances in functional and structural MR image analysis and implementation as FSL. *NeuroImage*, *23*(SUPPL. 1), 208–219. https://doi.org/10.1016/j.neuroimage.2004.07.051

Stevens, F. L., Hurley, R. A., & Taber, K. H. (2011). Anterior cingulate cortex: Unique role in cognition and emotion. *Journal of Neuropsychiatry and Clinical Neurosciences*, *23*(2), 121–125. https://doi.org/10.1176/jnp.23.2.jnp121

Strait, C. E., Blanchard, T. C., & Hayden, B. Y. (2014). Reward value comparison via mutual inhibition in ventromedial prefrontal cortex. *Neuron*, *82*(6), 1357–1366. https://doi.org/10.1016/j.neuron.2014.04.032

Tervo, D. G. R., Kuleshova, E., Manakov, M., Proskurin, M., Karlsson, M., Lustig, A., Behnam, R., & Karpova, A. Y. (2021). The anterior cingulate cortex directs exploration of alternative strategies. *Neuron*, 1–12. https://doi.org/10.1016/j.neuron.2021.03.028

Wang, X.-J. (2002). Probabilistic Decision Making by Slow Reverberation in Cortical Circuits. *Neuron*, *36*, 955–968. https://doi.org/10.1007/s00520-017-3845-y

Wang, X. J. (2012). Neural dynamics and circuit mechanisms of decision-making. *Current Opinion in Neurobiology*, *22*(6), 1039–1046. https://doi.org/10.1016/j.conb.2012.08.006

Wessel, J. R., Danielmeier, C., Bruce Morton, J., & Ullsperger, M. (2012). Surprise and error: Common neuronal architecture for the processing of errors and novelty. *Journal of Neuroscience*, *32*(22), 7528–7537. https://doi.org/10.1523/JNEUROSCI.6352-11.2012

Wilson, R. C., Geana, A., White, J. M., Ludvig, E. A., & Cohen, J. D. (2014). Humans use directed and random exploration to solve the explore-exploit dilemma. *Journal of Experimental Psychology: General*, *143*(6), 2074–2081. https://doi.org/10.1037/a0038199

Wittmann, M. K., Kolling, N., Akaishi, R., Chau, B. K. H., Brown, J. W., Nelissen, N., & Rushworth, M. F. S. (2016). Predictive decision making driven by multiple time-linked reward representations in the anterior cingulate cortex. *Nature Communications*, *7*(1), 1–13. https://doi.org/10.1038/ncomms12327

Woolrich, M. W., Behrens, T. E. J., Beckmann, C. F., Jenkinson, M., & Smith, S. M. (2004). Multilevel linear modelling for FMRI group analysis using Bayesian

inference. *NeuroImage*, *21*(4), 1732–1747. https://doi.org/10.1016/j.neuroimage.2003.12.023

Yamada, H., Louie, K., Tymula, A., & Glimcher, P. W. (2018). Free choice shapes normalized value signals in medial orbitofrontal cortex. *Nature Communications*, *9*(1), 1–11. https://doi.org/10.1038/s41467-017-02614-w

Zajkowski, W., Kossut, M., & Wilson, R. C. (2017). A causal role for right frontopolar cortex in directed, but not random, exploration. *Proceedings of ICCM 2017 - 15th International Conference on Cognitive Modeling*, 79–84. https://doi.org/10.1101/127704